DEPARTAMENTO DE CIÊNCIAS DA VIDA

FACULDADE DE CIÊNCIAS E TECNOLOGIA
UNIVERSIDADE DE COIMBRA

Cardiolipin Content in P19 Embryonal Carcinoma Cells

Dissertação apresentada à Universidade de Coimbra para cumprimento dos requisitos necessários à obtenção do grau de Mestre em Bioquímica, realizada sob a orientação científica do Doutor Paulo Oliveira (Centro de Neurociências e Biologia Celular) e da Professora Doutora Paula Verissímo (Departamento de Ciências da Vida, Faculdade de ciências e Tecnologias, Universidade de Coimbra).

Sílvia Carina Magalhães Novais

2014

This work was performed in the MitoXT: Mitochondrial Toxicology and Experimental Therapeutics laboratory at the CNC - Center for Neuroscience and Cell Biology. University of Coimbra.

The work presented was conducted under the guidance of Paulo Oliveira, PhD and Ignacio Vega-Naredo, PhD, Center for Neurosciences and Cell Biology, Coimbra Portugal.

This master thesis was performed under the academic supervision of Paula Veríssimo, PhD, Department of Life Sciences, University of Coimbra.

The present work was funded by the Portuguese Foundation for Science and Technology (FCT) (PTDC/QUI-BIQ/101052/2008 and PEst-C/SAU/LA0001/2013-2014) and co-funded by COMPETE/FEDER/ National Budget

The work was also supported by QREN project # 4832, reference 'CENTRO-07-ST24-FEDER-002008'.

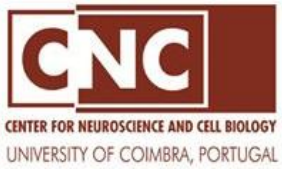

I declare that this is a true copy of my thesis including any final revision as approved by my supervisors and the Graduate Studies Office, and that this thesis has not been submitted for a higher degree to any other University or Institution.

Sílvia Carina Magalhães Novais

August 2014

ACKNOWLEDGEMENTS

I would like to start by thanking the Portuguese Foundation for Science and Technology for the research grants that financially supported the work in our laboratory.

I would like to thank to Doctor Paulo Oliveira, for all the help and support during my time in the lab. I am thankful for the opportunity that has been given to me.

I am also really grateful to Ignacio Vega-Naredo for his constant advice and guidance along this year. Under his guidance I successfully overcame difficulties and learned a lot.

I would like to thank to all colleagues in the lab, for all support with “the young ones”, to Doctor Sancha and Professor Moreno for their availability in all occasions and numerous efforts to successfully help getting the required resources for work, and in special to “dona” Paula for her dedication and support in the laboratory.

I thank Renata, João, Sales and Rita for their friendship, support and more importantly for making the writing of this thesis a lot more enjoyable. Thank you for share this moment in my life.

Finally, I would like to thank to my family, special to my parents and grandparents, for their love, encouragement and for always believing in me.

Gostaria de agradecer à minha família, em especial aos meus pais e avós, pelo amor, força, motivação e por sempre acreditarem em mim. A vós o meu muito obrigado.

CONTENTS

LIST OF FIGURES

LIST OF TABLES

ABSTRACT

The evolution of the carcinogenic process requires the knowledge of physiology and metabolism of cancer stem cells (CSCs), which seems be crucial for the development of novel effective therapies. In order to understand this process, mitochondria are unequivocally a target for cancer therapy and crucial in cell death. Given the relevance of mitochondrial metabolism for stemness maintenance, mitochondrial control of apoptosis and the importance of cardiolipin (CL) for mitochondrial metabolism, we proposed the study CL alterations during CSCs differentiation, so that CSCs resistance to therapies can be better understood. Our results indicate that, although the total content of CL did not significantly changed, CL remodeling, possible mediated by increased of taffazin and CLS amount, may lead to a metabolic transformation towards the typical oxidative metabolism that occurs during the differentiation of P19 CSCs. Differences in CL molecular species were observed with incorporation of oleic acid into CL from P19 CSCs. Moreover, the differentiation of P19 CSCs increased the peroxidation of CL. In a secondary objective of this work was to verify whether melatonin could affect P19 CSC proliferation. The results indicated that melatonin was only effective in reducing the proliferation of P19 cells with higher oxidative metabolism and was able to prevent CL peroxidation. Likewise, in cells with active oxidative metabolism, melatonin triggered a type of mitochondrial cell death which was mediated by the apoptosis-inducing factor (AIF). We conclude that the metabolic remodeling during P19 CSCs differentiation probably also involves alteration in CL metabolism that probably contributes in converting differentiated cells more susceptible to mitochondrial-targeted antitumor agents.

Keywords: Cardiolipin, remodeling, cancer stem cells, melatonin

SUMÁRIO

A evolução do processo carcinogénico requer o conhecimento da fisiologia e metabolismo das células estaminais de cancro (CEC) crucial para o desenvolvimento de novas e eficazes terapias. Uma vez reconhecido o seu importante papel no processo de morte celular, as mitocôndrias são inequivocamente um alvo promissor na terapia anti-tumoral. Dada a relevância do metabolismo mitocondrial na manutenção da pluripotência das células estaminais e a importância da cardiolipina (CL), no metabolismo mitocondrial, propusemos o estudo das alterações na CL durante a diferenciação de CEC de forma a entender a sua resistência a terapias. Os nossos resultados indicam que, embora o conteúdo total de CL não se tenha alterado de forma significativa, a remodelação da CL acompanhou a transformação metabólica em função do típico metabolismo mais oxidativo que ocorre durante a diferenciação de P19 CEC. Diferenças nas espécies moleculares CL foram observadas com a incorporação de ácido oleico na CL nas P19 CEC. Adicionalmente foi observado um aumento na peroxidação da CL durante a diferenciação das CEC. Um segundo objetivo deste trabalho foi verificar se a melatonina poderia afetar a proliferação das CEC P19. Os resultados indicaram que a melatonina, induziu uma redução na proliferação de células com maior metabolismo oxidativo e foi capaz de prevenir a peroxidação de CL em células diferenciadas. Do mesmo modo, em células com o metabolismo oxidativo ativo, a melatonina provocou um tipo de morte celular mitocondrial mediada por um fator indutor de apoptose. Concluímos assim que a remodelação metabólica durante a diferenciação de CEC P19, pode envolver alterações no metabolismo da CL que possivelmente contribuem para aumentar a suscetibilidade das células diferenciadas a agentes anti-tumorais direcionadas à mitocôndria.

Palavras-chave: Cardiolipina, remodelação, células estaminais de cancro, melatonina

LIST OF ABBREVIATIONS

ADP – Adenosine diphosphate

AIF – apoptosis inducing factor

ATP – Adenosine trisphosphate

BAX – BCL-2 associated X protein

BCA – Bicinchoninic acid

BCL-2 – B-cell CLL/lymphoma

BHT – Butylated hydroxytoluene

BSA – Bovine serum albumin

CEC – células estaminais de cancro

CL – Cardiolipin

CLS1 – Cardiolipin synthase 1

CSCs – Cancer stem cells

DCA – Dichloroacetate

dCCs – Differentiated cancer stem cells

dH_2O – deionized water

DMSO - Dimethyl sulfoxide

DNA – deoxyribonucleic acid

DTNB – 5,5'-Dithiobis-(2-Nitrobenzoic Acid)

DTT – Ditiotreitol

EC – Embryonal carcinoma

ECF – Enhanced Chemi-Fluorescence

EDTA – Ethylenediaminetetraacetic acid

ETC – electron transport chain

FA – fatty acid

FBS – fetal bovine serum

Gal-CSCs – cancer stem cells cultured in galactose medium

Gal-dCCs – differentiated cancer cells cultured in galactose medium

Glu-CSCs – cancer stem cells cultured in glucose medium

Glu-dCCs – differentiated cancer cells cultured in glucose medium

H_2O_2 – hydrogen peroxide

HCl – hydrogen chloride

HEPES – hydroxyethyl piperazineethanesulfonic acid

HPLC – High-performance liquid chromatography

KCl – Potassium chloride

KDa – kiloDalton

KH_2PO_4 – Monopotassium phosphate

MDA – malandolyl acid

MLCL – Monolysocardiolipin

MS – mass spectrometry

mtDNA – mitochondrial deoxyribonucleic acid

Na_2HPO_4 – Disodium phosphate

NaCl – sodium chloride

NAO – 10-*N*-nonyl acridine Orange

OXPHOS - Oxidative phosphorylation

PA – phosphatidic acid

PBS – Phosphate buffered saline

PC – phosphatidylcholine

PDH – pyruvate dehydrogenase

PDK – Pyruvate dehydrogenase kinase

PE – phosphatidylethalonamine

PG – phosphatidylglycerol

PI – phosphatidylinositol

PIC – protease inhibitor cocktail

PL – phospholipid

PLA_2 – Phospholipase A_2

PMSF – Phenylmethanesulfonyl fluoride

PS – Phosphatidylserine

RA – Retinoic acid

ROS – Reactive oxygen species

SDS – sodium dodecyl sulfate

SDS–PAGE – sodium dodecyl sulfate polyacrylamide gel

SRB – sulforhodamine B assay

TLC – thin-layer chromatography

TOM20 – translocase of outer mitochondrial membrane 20 homolog

PART 1

GENERAL INTRODUTION

1.1 - Stem Cells and Cancer Stem Cells

Stem cells are defined as undifferentiated cells with self-renewal potential that are able to differentiate into a large number of diverse mature progeny. Amongst the various categories of stem cells, embryonic stem cells are pluripotent and are able to differentiate into any cell type due to the influence of microenvironmental and some other factors such as microRNAs expression[1], making them a very promising foundation for stem cell-based therapeutics[2]. Stem cells can divide asymmetrically producing two daughter cells – one being a new stem cell and the second a progenitor cell, which has the ability for differentiation and proliferation, but without self-renewal potential. Stem cells can also divide symmetrically resulting in two cells equal to itself with essentially the same development and replication potential, keeping a constant pool of stem cells.

Similarly to organs, tumors are composed of a mixture of cells at varying states of differentiation and arise from cells with the ability to proliferate indefinitely and differentiate into multiple lineages of cells[3,4]. In healthy tissues, stem cells are responsible for organ development, suggesting that tumors also have a subset of cells with stem-like characteristics known as cancer stem cells[3]. Over the past decade, support for the existence of cancer stem cells has grown, suggesting that cancer stem cells are a driving force in tumorigenesis.

Cancer development and maintenance can be explained by two different models: the cancer stem cell model and the clonal evolution model[5] (Figure 1). The cancer stem cells model presumes that tumor progression is a result of the metastatic spread of these cells tumorigenic, which are relatively more slow-growing or quiescent, and then relatively more resistance to therapy[4]. On the other hand, the clonal evolution model or the stochastic model proposes that any tumor cell has the potential to be involved in tumor progression and consequentially becoming invasive and also resistant to therapies[5].

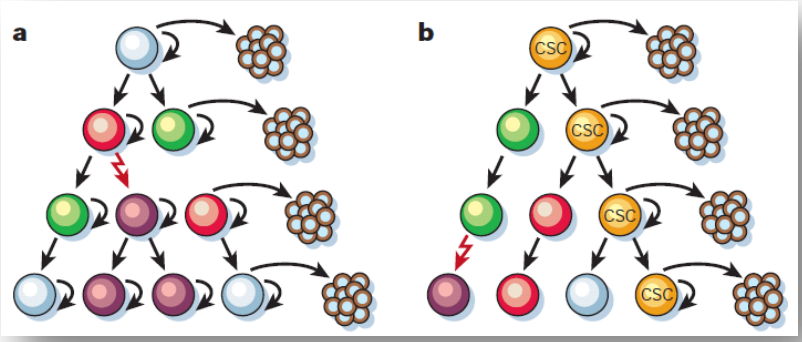

Figure 1.1 - Two general models to explain heterogeneity in solid cancer cells. a. Stochastic clonal evolution model: cancer cells of many different phenotypes have the potential to proliferate extensively, but any single cell would have a low probability of exhibiting this potential in an assay of clonogenicity or tumorigenicity. **b**, Cancer stem cell hierarchy model: most cancer cells have limited proliferative potential and only a subset of cancer cells consistently proliferate extensively in clonogenic assays and can form new tumors on transplantation. (Taken from *Reya et al.* [3] with permission – Appendix 1)

Cancer stem cells, described above, can derive from adult stem cells in various developed tissues, but also from early embryonic stem cells. This category of cancer stem cells are known as embryonal carcinomas (EC). EC cells are the stem cell subpopulation of a category of malignant germ cell tumors known as teratocarcinomas[6]. In fact, recently it was proposed that P19 EC cells can provide an important cell model to study the differentiation and chemoresistance in cancer stem cells[3]. P19 cells are derived from a teratocarcinoma formed by transplantation of a 7.5 day embryo into the testis[7]. The development of P19 EC cell lines was a result from the establishment of cell lines using female embryos which were heterozygous for X-linked P19 EC alleles[7]. For this purpose, 7.5-day-old embryos derived from crossing a C3H/He female with males carrying an X-chromosome derived from a feral mouse bearing a number of variant alleles, were transplanted into the testis of a C3H/He mouse receptor. Undifferentiated P19 EC cells derived from the primary tumor have a euploid karyotype and grow rapidly in culture without the need for feeder cells (Figure 1.2 A,B,C).

An efficient differentiation of P19 EC cells depends on whether the cells are cultured is at a high density[8] or if they form aggregates[9] (Figure 1.4 D,E,F). The compounds most effective in inducing differentiation of P19 cells are retinoic acid (RA)[10] and dimethyl sulfoxide (DMSO)[8]. Both compounds are not demonstrably toxic

to P19 cells at the doses effective in inducing differentiation, indicating that their effect is true induction and not selection of pre-existent differentiated cells[11,12]. The precise effect induced by RA seems to be variable depending on the particular cell line used and on whether or not cells are exposed to the agent as aggregates or in monolayer. At the dose of RA normally used ($3x10^{-7}$ M), neurons are the first and most abundant cell type resulting from P19 cells growing as spheroids [10]. Also, oligodendrocytes can be originated from RA-treated cells although this differentiation has only been observed in P19 cells grafted into the brains of neonatal rats[13]. At least three days after RA treatment, the first markers of differentiated neurons appear, confirming that RA has an important role in signaling pathways that culminates in cellular differentiation[14].

The site of RA action appears to be a group of nuclear retinoic acid receptors (RARs) that are known to be ligand-dependent transcription factors[15]. Binding of RA to RARs alters the conformation of the RARs, which affects the binding of other proteins that either induce or repress transcriptional activity of nearby genes (including Hox genes and several other target genes)[16]. Retinoic acid receptors mediate the transcription of different sets of genes controlling differentiation of a variety of cell types. Other agent that induces P19 EC cells differentiation into all three germ layers is DMSO. About 0.5–1% DMSO efficiently induces P19 cell aggregates to develop into a wide variety of mesodermal and endodermal cell types[14,17] including cardiac and skeletal muscle, epithelium and other uncharacterized cells. Treatment P19 EC cells or other cells types with DMSO, leads to an increase in intracellular calcium released from intracellular stores, which could trigger crucial events for cardiac muscle differentiation[18]. However, the molecular events that occur during aggregation and that are necessary for cardiac differentiation are not yet fully understood.

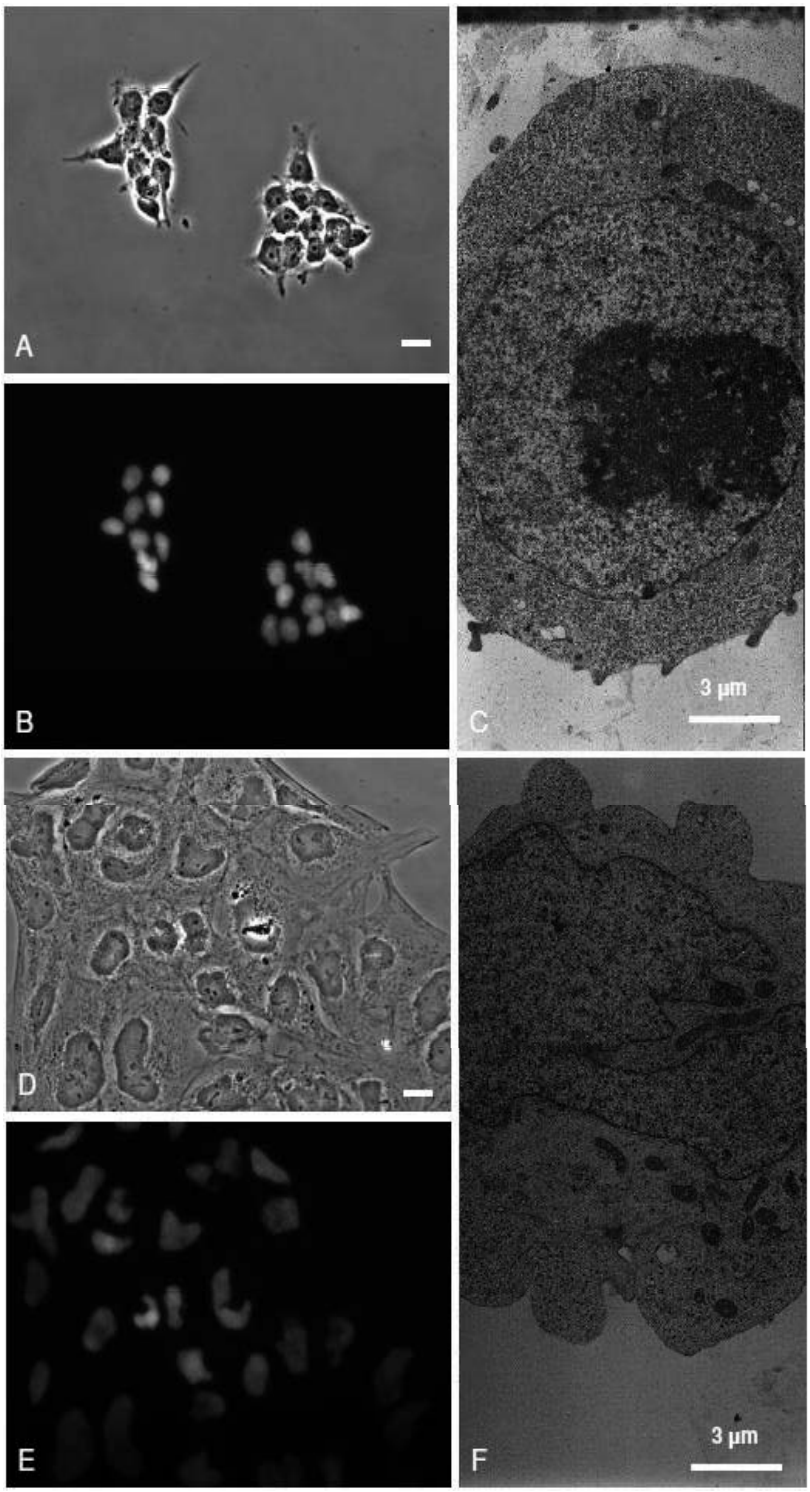

Figure 1.2 - Characteristics of P19 stem cells (P19SCs) versus differentiated cells (P19dCs). Imaged by epifluorescence microscopy with Hoechst labeling for nuclear staining and electron microscopy. Detailed photographs of nuclei (A, B) and nucleolus (C) present in P19SCs. E and F represent nuclei and visible heterochromatin in P19dCs respectively. Bars = 15 µm (A, B, D, E) and 3 µm (C, F). (Taken from I, Vega-Naredo *et. al.* [8] with permission – Appendix 2)

The critical problem in the development of anti-cancer therapies is effectively the presence of different groups of cells in tumor bulb. For this reason most of the usual therapies anti-cancer has their action failed in some tumors. In the conventional view of drug resistance, one or several cells in the tumor population acquire genetic changes that confer drug resistance[19]. These cells have a selective advantage that allows them to overtake the population of tumor cells following cancer chemotherapy. After selection for resistance to a single drug, cells may also show cross-resistance to other structurally and mechanistically unrelated drugs — a phenomenon that is known as multidrug resistance[20], which explain why treatment regimens that combine multiple agents with different targets are not more effective[19]. Cancer stem cells resistance to standard chemotherapeutics has been reported in human leukemia[21] malignant melanoma[22], brain[23], and breast[24] cancer. Furthermore cancer stem cells resistance to radiotherapy has also been reported in some brain[25] and breast[26] cancers.

Several hypotheses have been proposed to account for the phenomenon of drug resistance. The hypotheses include the increased expression of anti-apoptotic BCL-2 family members, alteration of drug transport across the plasma membrane, as consequence of the ABC-transporter over-expression, activation of DNA repair mechanisms, and alteration in target molecules[19]. The main mechanism underlying the ability of CSCs to resist chemotherapy is the inhibition of apoptosis. Apoptosis is a regulated process by which a cell undergoes programmed death, resulting in fragmentation of the cell into membrane-bound particles that eventually are phagocytosed by specialized cells. A key signaling phenomenon responsible for triggering the cascade of events that precedes cell death is the release of cytochrome c from the inter-membrane space. Cytochrome c activates proteins responsible for executing the apoptotic program-caspases cascade. The mitochondrial apoptotic pathway is in turn regulated by members of the Bcl-2 family[27] including pro-apoptotic p53 transcriptional targets like Bax, Bak, Noxa, and PUMA[28] and anti-apoptotic members such as Bcl-2 and Bcl-xl[28]. Thus, cancer cells with Bax depletion are resistant to mitochondria-mediated apoptosis[29] and overexpression of exogenous Bcl-xL or Bcl-2 suppresses apoptosis[30]. On the other hand, downregulation of Bcl-xL or Bcl-2 can enhance the apoptotic response to DNA damage, but in a p53- and Bax-dependent manner. Another significant mechanism of resistance against a variety of anti-cancer

drugs is through the action of a group of membrane proteins which excludes cytotoxic molecules, keeping intracellular drug concentration below a cell-killing threshold. The first of these carriers to be identified and characterized was P-glycoprotein (also known as MDR1), which is a member of the superfamily of ABC transporters (ATP-binding cassette), that is encoded by the ABCB1 gene[31]. Tumors with MDR protein overexpression[32,33,34] frequently show intrinsic resistance[35]. However, the action of some therapies can be altered by the modification of its target and then their therapeutic potential influenced[36]. This way, the cell has no longer a known useful target to block.

Due to the CSCs resistance to chemotherapy, novel therapeutic approaches have been designed with the aim of killing CSCs and altering the microenvironment supporting these cells. Some these approaches include cellular markers as CD133 (also known as Prominin1)[37], CD44, CD24, epithelial cell adhesion molecule (Ep- CAM), THY1 and ATP-binding cassette B5 (ABCB5)[38]. Some therapies using CD133 and/or EpCAM and ABCC5 antibodies to prevent tumor progression and metastasis are being tested in different clinical trials[39,40,41] .

1.2 – Mitochondria in cancer stem cells

Mitochondria play a relevant role in the cellular metabolism and for coordinating extrinsic and intrinsic signals which direct cell growth, proliferation differentiation, and death[42,43]. Dysfunction in the mitochondrial machinery has a major role in aging and apoptosis and contributes for many diseases including cancer. There are several processes associated to mitochondria that allow distinguishing cancer cells from normal healthy cells such as an increase in membrane potential associated to a decrease of mitochondrial ATP production and increased glycolytic ATP production[44]. In fact, the fast-growing of tumor cells are characterized by a high glycolytic activity, even in the presence of saturating oxygen, the so-called Warburg effect[45]. Warburg proposed that neoplastic cells undergo a metabolic shift from aerobic respiration to aerobic glycolysis, involving lactic acid fermentation, which would occur even at normal oxygen tensions. Moreover, he also proposed that cancer cells rely on less efficient aerobic glycolysis to achieve their energy requirements due to defects in the oxidative phosphorylation metabolic pathway[45]. In fact, despite the presence of functionally competent

mitochondria, the allosteric modulation of glycolytic enzymes in tumor cells prevents mitochondrial ATP production[46] whereby non-tumor cells normally rely on aerobic respiration which makes use of both cytosolic and mitochondrial processes to generate energy. Contrarily, the glycolytic profile of the CSCs seems to be consequence of reduced mitochondrial activity, yet have low rates of O_2 consumption that accurately reflect their lack of reliance on OXPHOS for energy production.

Mitochondria have been shown to change in number, structure and physiological function with cell differentiation[47]. Studies investigating mitochondrial changes in neuronal differentiation of P19 EC cells have reported increases in mitochondrial mass with differentiation in both existing studies. Conflicting results were reported for mtDNA copy number[48] with unchanged mitochondrial mass and mtDNA during RA-induced P19 EC cell differentiation[49]. Previous results from our laboratory showed that in comparison with their differentiated counterparts, pluripotency of P19SCs was correlated with a strong glycolytic profile, decreased mitochondrial biogenesis and complexity. Indeed, low-polarized and inactive mitochondria with a closed permeability transition pore were observed in P19SCs (Figure 1.3). Furthermore when P19SCs were differentiated with RA, they lost pluripotency while retaining their immortality and some stem-like properties. The decreased mitochondrial capacity observed in P19SCs was related to increased resistance against dichloroacetate[49]. Dichloroacetate (DCA), a mitochondria-targeting small molecule, has been shown to reverse the abnormal metabolism of cancer cells by shifting it from glycolysis to glucose oxidation through inhibition of pyruvate dehydrogenase kinase (PDK)[50]. DCA indirectly stimulates conversion of pyruvate to acetyl-CoA and up-regulates mitochondrial metabolism[51]. Dichloroacetate is also reported to reduce proliferation, increase apoptosis and to suppress tumor growth by normalizing mitochondrial function[51,52]. Thus, stimulation of mitochondrial function by growing P19SCs in glutamine/pyruvate-containing medium decreased their glycolytic phenotype, inducing loss of pluripotent potential, compromising differentiation and became P19SCs sensitive to DCA.

Because of the central role of this type of stem cells in teratocarcinoma development, those findings highlight the importance of mitochondrial metabolism in stemness, proliferation, differentiation and chemoresistance.

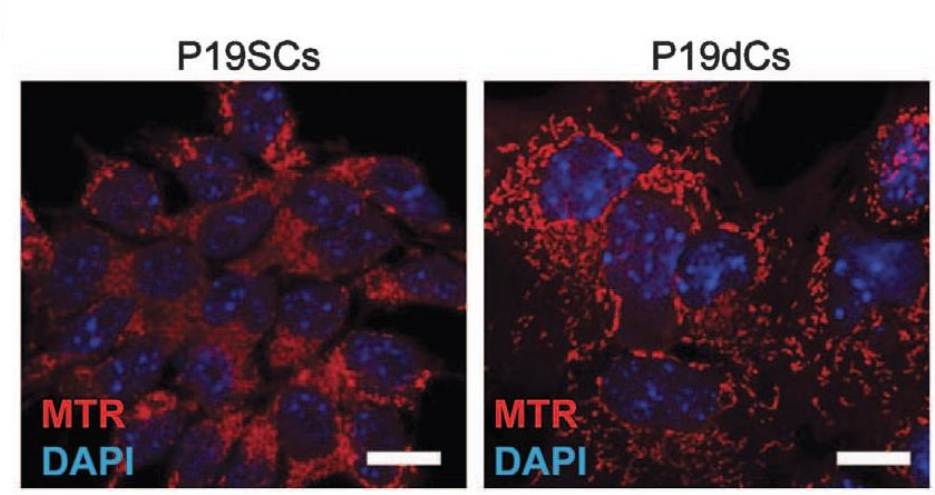

Figure 1.3 – Alterations in mitochondrial morphology during P19SCs differentiation retinoic acid-induced. Confocal images obtained using MitoTracker Red (MTR) or TMRM for mitochondrial labeling and DAPI or Hoechst for nuclear labeling show alterations in mitochondrial morphology between P19SCs and P19dCs, growing in monolayer and in spheroids (3D) (Taken from I, Vega-Naredo *et. al.* [8] with permission – Appendix 2)

1.3 – Cardiolipin

Cardiolipin (CL) is one of the most important phospholipid in mitochondrial membranes. CL was first isolated from beef heart[53], and due its particular structure, it has been subjected to numerous investigations. In mammalian tissues, CL is characteristically associated with the inner mitochondrial membrane[54] and is intimately associated with, a number of key mitochondrial enzymes including cytochrome c oxidase, ATP/ADP exchange protein, FoF1 ATP synthase and cytochrome bc1 complex[55].

1.3.1 - Cardiolipin biosynthesis

Cardiolipin is synthesized in a series of steps from phosphatidic acid ans is remodeled into a form which, in the heart, is rich in linoleic acid (18:2). In mammalian

tissues, CL biosynthesis occurs via the cytidine diphosphate-diacylglycerol (CDP-DG) pathway (Figure 1.4). In the first step of this pathway phosphatidic acid (PA) and cytidine 5-triphosphate (CTP) are converted to CDP-DG; then, the conversion of CDP-DG and glycerol 3-phosphate to phosphatidylglycerol (PG) occurs by the sequential action of phosphatidylglycerol phosphate (PGP) synthase and PGP phosphatase. In the final step of the pathway, PG is then converted to CL via condensation with CDP-DG catalyzed by CL synthase. Newly synthesized PA and PG may be preferentially utilized for CL biosynthesis in the heart[56]. In addition, separate pools of PG, including an extra-mitochondrial pool not derived from new phosphatidylglycerol biosynthesis, may be utilized for cardiac CL biosynthesis. After the remodeling of the four saturated acyl chains of CL synthesized, more unsaturated fatty acyl chains are incorporated given to the CL a high degree of symetry[57]. Tafazzin, the gene product of TAZ1, is a key player in the remodeling of newly synthesized CL, functioning as a monolysocardiolipin (MLCL) transacylase[58]. The remodeling is initiated by a phospholipase, which is identified in mammalian cells as phospholipase A2 (PLA2), an enzyme that supply the lysocardiolipin acceptor substrate for acylation/transacylation remodeling reactions necessary for the generation of symmetric tetra-18:2 CL molecular species[59]. Furthermore, it was observed that the accumulation of MLCL, resulted from impaired taffazin activity, can compromise the remodeling of CL even the process was already initiated[59]. On the other hand, the catabolism of CL may occur by the catalysis of phospholipase A2 which removes fatty acyl groups or by phospholipase D which hydrolyses CL to PA.

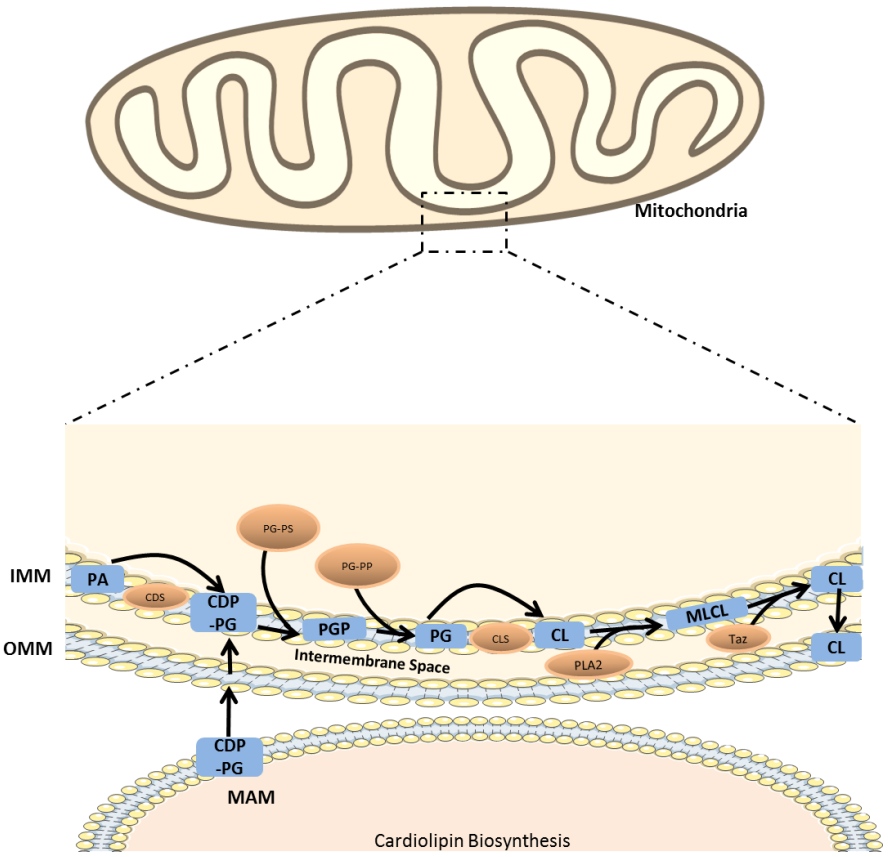

Figure 1.4 - Pathways of cardiolipin (CL) biosynthesis and remodeling, in mammalian cells. See text for details. CDP-DAG, cytidinediphosphate-diacylglycerol; CDS, CDP-DAG synthase; CS, CL synthase; DLCL, dilyso-CL; MLCL, monolyso-CL; MLCLAT, MLCL acyltransferase; PG, phosphatidylglycerol; PG-P, PG phosphate; PGPP, PG-P phosphatase; PGPS, PG-P synthase; PLA2, phospholipase A2; TA, transacylase.

1.3.2 - Role of cardiolipin in mitochondria

The exclusive presence of CL in bioenergetics membranes allows its interactions with the electron transport chain complexes involved in oxidative phosphorylation. Indeed, CL is required for optimal activity of complex I (NADH dehydrogenase), complex II (Succinate dehydrogenase), complex IV (cytochrome c oxidase) and complex V (ATP synthase), four large complexes integrated in the inner mitochondrial membrane[60]. It was also proposed that cytochrome c release from mitochondria requires first the dissociation of its interactions with CL[61], triggering the downstream events in apoptosis. This peculiar phospholipid can also have a very important role in different pathologies, particularly in Parkinson and Alzheimer diseases, in which the content of CL decreases with age[62], in heart failure[63], in diabetes[64], in cancer[65], and in Barth syndrome, a rare and often fatal X-linked genetic disease that is associated with

cardiomyopathy[66]. Barth syndrome is associated to a mutation in the gene coding for tafazzin. Mutations in tafazzin results in abnormal CL species which leads to ATP depletion and finally could affect the function of the cardiomyocytes.

Oxidative stress and lipid peroxidation have been associated with several diseases and disorders. The abundance of double bonds in its structure turns CL more susceptible to peroxidation[67], and its close association with respiratory chain proteins, are known to be a major source of reactive oxygen species (ROS) in mitochondria[68,69]. In fact, numerous studies indicate that peroxidized CL is unable to support the reconstituted activity of mitochondrial respiratory enzymes[68,70,71]. The pathological consequences of CL compositional changes have been associated to shifts in acyl chain remodeling pathway (Figure 1.2) Indeed, a reduction in the bioavailability of 18:2, essential fatty acid, or alterations in the activity or acyl-specificity of putative CL remodeling enzymes may result in aberrant CL. The acyl composition of CL is well known to be sensitive to FA composition of the diet which could result in mitochondrial respiratory dysfunction[72]. Hence, the involvement of CL in the mitochondrial enzymes activity and apoptosis mechanisms converts this phospholipid in an important component to study the mechanisms of resistance in cancer stem cells.

1.4 - Melatonin

Melatonin (N-acetyl-5-methoxytryptamine), the main pineal hormone, can also be produced in many other organs and tissues[73]. Its hydrophilic and lipophilic characteristics allow melatonin to reach any cell, compartment or body fluid[74]. It is involved in a variety of physiological functions, including modulation of gene transcription[75], blockage of transcriptional factors[76] and control of mitochondrial activities[77]. Melatonin attenuates oxidative stress acting as a direct free radical scavenger and stimulating the activity and expression of antioxidant enzymes[78,79]. In addition to controlling redox metabolism and circadian and seasonal rhythms, many other functions have been attributed to melatonin: influences immune system[80] modulates mitochondrial activity[77] cell death[81] and autophagy[82], and presents antitumoral properties[83]. Melatonin exerts strong anti-tumor activity via several mechanisms, including anti-proliferative and pro-apoptotic effects in addition to its

potent antioxidant activity. On mitochondria from normal cells, the physiological effects of melatonin are mainly to prevent mitochondrial impairment, energy failure, and apoptosis in oxidatively-damaged mitochondria[77] what could provide a new homeostatic mechanism regulating mitochondrial function. Despite this array of information, there are studies regarding the effects of melatonin on CSCs in different stages of differentiation.

PART 2

OBJECTIVES

Given the relevance of mitochondrial metabolism for stemness maintenance, the mitochondrial control of apoptosis and the importance of cardiolipin for mitochondrial function and dysfunction, the study of cardiolipin in during CSCs differentiation is of great interest for understanding their resistance to therapies.

Therefore, the main objective of the present work was to examine cardiolipin remodeling during the differentiation of P19 stem cells under different metabolic conditions to understand if cardiolipin alterations occur during cell and metabolic remodeling toward a more oxidative condition.

In addition, since the effects of melatonin in cancer cells expressing stem cell-like characteristics are not known, we also analyzed the effects of this indolamine in the P19 CSCs model, when administered alone or in combination with DCA.

PART 3

MATERIALS AND METHODS

3.1 - Reagents and kits

Reagents used in cell culture, such as 0.05% Trypsin-EDTA (25300-062) and fetal bovine serum (FBS; 16000-044) were purchased from Invitrogen (Carlsbad, CA, USA) while Dulbecco's modified Eagle's medium (DMEM) -high glucose (D5648), sodium bicarbonate (S5761), sodium pyruvate (P5280), galactose (G5388), glutamine (G3126) and antibiotic/antimycotic solution (A5955), retinoic acid (R2625) as well as DMEM free-glucose (D5030) and trypan blue (T8154) were obtained from Sigma, (St. Quentin Fallavier, France). The standards polar lipids used in the separation of the different classes of phospholipids were obtained from Avanti Polar Lipids, Inc (Delfzyl, The Netherlands). The RIPA buffer used for total protein harvesting was purchased from Thermo Fisher and PIC (P8340), PMSF (P7626) and DTT (D9779) were obtained from Sigma Sigma-Aldrich (St. Louis, MO, USA). The protein quantification bicinchonic acid assay (BCA) was performed using the pierce BCA assay kit from Thermo Fisher Scientific (23250; Lafayette, CO, USA). Additionally, the Laemmli buffer was purchased from BioRad (161-0737; Hercules, CA, USA).

Agents used for citotoxicity assays such as hydrogen peroxide (121076) were purchase from Panreac, Barcelona, Spain, and melatonin (M5250) and dichoroacetate (347795) were acquired from Sigma-Aldrich (St. Louis, MO, USA).

Moreover, precision plus protein dual color (161-0374) molecular weight standard and the blotting-grade blocker non-fat dry milk (170-6404) were obtained from BioRad (Hercules, CA, USA). In addition, membrane protein detection was achieved using the Enhanced Chemi-Fluorescence system (ECF) from GE Healthcare (RPN3685; Buckinghamshire, UK). All primary antibodies used are listed in Table 3.1 as well as their respective catalog number and brand; the secondary antibodies used were all purchased from Santa Cruz Biotechnology (CA, USA).

Acridine Orange 10-nonyl bromide (NAO) was obtained from Sigma-Aldrich (A7847; St. Quentin Fallavier, France).

All general chemicals used were of the highest grade of purity commercially available.

3.2 - Cell culture

P19 embryonal carcinoma cells were obtained from the American Type Culture Collection (ATCC, CRL-1825) and cultured in glucose- or galactose (glucose free)-containing media at 37 ºC in a 5% CO_2 atmosphere. Cells were cultured in DMEM - high glucose supplemented with 10% FBS, 1.8 g/l sodium bicarbonate, 110 mg/l sodium pyruvate and antibiotic/antimycotic solution. Galactose (glucose-free) medium was prepared using DMEM without glucose supplemented with 10% FBS, 1,8 g/l sodium bicarbonate, 110 mg/l sodium pyruvate, 1.8 g/l galactose, 0.584 g/l L-glutamine and antibiotic/antimycotic solution. For routine subculturing, cells were first rinsed with 1x PBS (0.137 M NaCl, 2.7 mM KCl; 1.4 mM KH_2PO_4; 0.01 M Na_2HPO_4) and then incubated with 1 volume of trypsin-EDTA for 3 min at 37°C. Trypsin activity was inhibited by the addition of 1 volume of complete growth medium and the final volume centrifuged at 300 g for 3 min at room temperature. An appropriate aliquot of the cell suspension was added to new culture flasks to obtain cultures between $2x10^3$ and $1x10^4$ viable cells/cm^2. This procedure was repeated when cultures reached 80-90% confluence. Cells were used between passages 5 and 25.

3.4 - Cell differentiation and treatment

To initiate differentiation, P19 cells were seeded, in 100 mm dishes culture at a density of $5.2x10^3$ cells/cm^2 and 1 µM RA was added for 96 hours. The procedure was performed in absence of light to prevent loss of acid proprieties. The stock of RA (100mM) was prepared by the addition of DMSO. After differentiation, cells were seeded and allowed to grow for 24 hours before further experiments.

The cells were exposed, twenty-four hours after sedding, to 500 µM and 1mM H_2O_2 during 2, 4 and 6 hours. Melatonin was dissolved in ethanol and DCA in water. Twenty-four hours after seeding, cells were exposed to 0.1 mM and 1 mM melatonin alone or in combination with 10 mM DCA during 72 hours. Controls were always treated with the same amount of vehicle (less than 0.95 % ethanol).

3.5 - Lipid extraction

The cells were washed with ice-cold PBS, scraped into 5 mL ice-cold PBS, and cell pellet was obtained by centrifugation at 200g for 4 min. The final cell pellet was re-suspended in 1 mL dH_2O. Total lipids were extracted by the Bligh and Dyer method[84]. Briefly, 3.75 mL chloroform–methanol 1:2 (v/v) and a low amount of BHT (5 µg/ml) were added to the cell suspension, vortex the mixture well, and incubating on ice for 30 min. An additional 1.25 mL chloroform was then added and, finally, 1.25 mL dH_2O. After vigorous vortex mixing the samples were centrifuged at 1000 g for 5 min at room temperature to obtain a two phase system: the aqueous top phase and organic bottom phase from which lipids were obtained. The total lipid extracts, recovered from the bottom phase, were dried under N_2 gas and stored at −20 °C.

3.6 - Lipid separation

Total lipid extracts were separated into different classes by thin-layer chromatography (TLC). Several spots corresponding to 30 µg total lipid extract dissolved in chloroform were applied to a TLC plate. We used TLC plates with concentrating zone 20cm×20 cm, 0,65mm (Merck, Darmstadt, Germany). Before separation, plates were washed with chloroform-methanol and after drying sprayed with 2.3% boric acid in ethanol and subsequent exposure to high temperature (100ºC for 15 min). The plates were developed with chloroform–ethanol–water–triethylamine 30:35:7:35 (v/v) as mobile phase. Lipid spots on the silica plates were observed by spraying the plates with primuline (5mg/100ml) and identified (UV lamp at 260 nm) by comparison with authentic lipid standards. Then, classes from five spots were scraped off the plates: one spot was quantified with the phosphorus assay, and four spots were extracted with the use of chloroform/methanol (2:1) (v/v) for subsequent identification by mass spectrometry (MS).

3.7 - Phospholipids quantification

Phospholipids in lipid extracts or in chromatographic fractions were estimated by phosphorus determination through an acidic digestion. The released inorganic phosphate was reacted with ammonium molybdate, with the complex giving a strong blue color. To evaluate the phospholipid content, phosphorus assay was performed by a method described elsewhere[85]. Briefly, 500 µl perchloric acid (70%) was added to phosphate standards of KH_2PO_4 (1-5ug) and samples (25 µl; 50 µl and 100 µl) previously dried. The samples were incubated for 1 hour at 180 °C, followed by cooling to room temperature. Then, 3.3 ml of water, 0.3 ml ammonium molybdate, and 3.3 ml ascorbic acid were added to the standards and samples, which were then incubated for 10 min at 100 °C in a water bath. The classes from spots scraped to silica plates were centrifuged for 5 min at 1000 g to separate PLs from silica. Finally, the standards and samples solutions were measured at 800 nm. These experiments were performed at least in triplicate, from different cell culture obtained on different days. The relative abundance of each PL class was calculated by relating the amount of PL class with the total amount of PL in the sample.

3.8 - Silica extraction

In order to analyze the different phospholipid classes by mass spectrometry, TLC spots corresponding to all identified classes were scraped off from the plates with the help of a spatula to a piece of aluminum paper, and then transferred to a glass tube. Four hundred and fifty µL of chloroform was added of all tubes, vortexed well and left to stand for 5 min, in order to be able to extract the phospholipids from the silica. Then, samples, were filtered under vacuum with a sand plate funnel; 450 µL of chloroform/methanol 1:1 (v:v) were added to the tubes, vortex well and then filtered again. After each sample the filter was thoroughly washed with methanol, and was changed every two filtered samples. The filtered samples were dried under nitrogen flow and were re-suspended in 100 µL of chloroform to mass spectrometry analysis, or stored at -4ºC for further analysis.

3.9 - Electrospray mass spectrometry

Analysis of CL was carried out in negative modes on electrospray (ESI) linear ion trap mass spectrometer (ThermoFinnigan, San Jose, CA, USA), and electrospray triple quadrupole mass spectrometry (Walters, Manchester, UK). The samples for electrospray analysis were prepared by diluting in 20µl CL (obtained after extraction from silica and re-suspended in 100 µl of chloroform) with 200 µl of methanol.

The samples were introduced into the mass spectrometer using a flow rate of 8 µl/min. ESI conditions in electrospray linear ion trap mass spectrometer were also as follows:, voltage, 4.7 kV, capillary voltage -34.9 V, tube lens voltage -124.9 V, capillary temperature 275ºC, and the sheath gas flow was 25 units. Isolation with an interval of 0.5 Da was used with a 30 milliseconds activation time for MS/MS experiments.

Full scan MS spectra and MS/MS spectra were acquired with 50 and 200ms maximum ionization time. Normalized collision energy (CE) was varied between 17 and 20 (arbitrary units) for MS/MS. Data acquisition of this mass spectrometer was carried out using an Xcalibur data system (V2.0).

3.10 - Citrate synthase activity

Citrate synthase is the initial enzyme of the tricarboxylic acid (TCA) cycle and an exclusive marker of the mitochondrial matrix. The enzyme catalyzes the reaction between acetyl coenzyme A (acetyl CoA) and oxaloacetic acid to form citric acid. The hydrolysis of the thioester of acetyl CoA results in the formation of coenzyme A with a thiol group (CoA-SH) which when reacts with the DTNB form the 5-thio-2-nitrobenzoic acid (TNB) , which exhibits maximum absorbance at 412 nm.

After sonication, P19 cells (5 µg) were incubated in 0.9 ml of 50 mM potassium phosphate (pH 7.4) at 21 ºC in the presence of 100 µM DTNB and 100 µM acetyl CoA. The citrate synthase reaction was initiated by the addition of 100 µM oxaloacetate and monitored by the spectrophotometric, at 412 nm. The intensity of the absorbance is proportional to citrate synthase activity.

3.11 - Sulforhodamine B assay

This method is based in the ability of the bright pink aminoxanthene SRB dye with two sulfonic groups to bind to cell proteins under mildly acidic conditions[86]. Under these conditions, SRB binds to protein basic amino acid residues in acid-fixed cells to provide an estimate of total protein mass, which is related to cell number. Accordingly, this assay allows to indirectly accessing cell proliferation and viability. Moreover, once pH is alkalinized, basic amino acids became protonated and the SRB dye is released into the solution allowing its spectrophotometry measure.

P19 cells were seeded in in 48-well plates at a concentration of $0.5x10^4$ cells/ml for P19 CSCs and $2x10^4$ cells/ml for P19 dCCs. Twenty-four hours after seeding, cells were treated with hydrogen peroxide (H_2O_2) (500µM and 1mM). Following treatment (0h, 2h, 4h and 6h), the incubation media were removed and cells were fixed in 1% acetic acid in 100% ice-cold methanol for at least 2h at -20ºC. The cells were then incubated with 0.5% (wt/vol) SRB in 1% acetic acid for 1 h at 37°C, and subsequently washed three times with 1% acetic acid to remove unbound staining. Then, 500 µl of Tris 10mM, pH 10 was added and the plates were incubated at room temperature in orbital shaking platform for 30 min in order to solubilize bound-protein. Finally, 200µL of the solubilized solution was transferred to a standard 96-well plate and its absorbance read in a VITOR X3 microplate reader (Perkin Elmer, Waltham, MA, USA) working at room temperature with a 544/15 nm filter.

3.14 - Trypan blue dye exclusion assay

In this work, a trypan blue dye exclusion assay was performed to analyze the cell viability after treating cells with melatonin. Treated and control P19 cells were trypsinized and washed with PBS. The cell suspension (100 µl) was aseptically transferred to a 1.5 ml tube and an equal volume of trypan blue was added for 3 minutes at room temperature. The re-suspension was then placed in a dual-use counting slide (145-0011, Bio-Rad; Hercules, CA, USA) and read in a TC20 automated cell counter (145-0102SP, Bio-Rad).

3.12 - Protein Quantification

Protein was quantified using the bicinchoninic acid assay (BCA) following manufacturer instructions. Working Reagent was prepared in a proportion of 50 parts of BCA reagent A to 1 part of reagent B. The reaction was initiated by adding 200 µL of working reagent to 8 µL of sample diluted 1:5 in ultrapure water, in a standard polystyrene flat bottom 96-well microplate. After 30 min incubation at 37°C, absorbance was read in a VICTOR X3 plate reader (Perkin Elmer Inc.) using a 544/15 nm filter. The standard curve ranging from 25 to 2000 µg/ml was made using a solution of BSA standard vials included in the referred kit. Standards and unknown samples were performed in duplicates.

3.13 - Western blot analysis

In order to obtain total cellular extracts, P19 cells were harvested by trypsinization, washed with PBS and centrifuged for 5 min at 1000 g. The cellular pellet was re-suspended in RIPA buffer supplemented with 2 mM DTT, 100 µM PMSF, and a protease inhibitor cocktail (containing 1 µg/ml of leupeptin, antipain, chymostatin, and pepstatin A), physically ruptured by sonication and kept at -80 ºC until used.

After protein quantification, samples were diluted in a Laemmli buffer (62.5mM Tris pH 6.8 (HCl), 2% SDS, 50% Glycerol, 5% β-mercaptoethanol, 0.04% bromphenol blue). Protein lysates were then boiled at 95ºC for 5 min. The previous steps led to protein denaturation and therefore loss of quaternary, tertiary and secondary protein structure allowing separated solely as a function of their molecular size. The separating gel consisted in 12% acrylamide/bis, 375mM Tris pH 8.8 (HCl), 0.1% SDS, 0.05% TEMED and 0.05% APS while stacking gel consisted in 4% acrylamide/bis, 126mM Tris pH 6.8 (HCl), 0.1% SDS, 0.1% TEMED and 0.05% APS. Different final acrylamide/bis percentages were used depending on the molecular size of the proteins of interest allowing a maximum separation resolution.

Equivalent amounts of protein (25-50 µg) were separated by electrophoresis using a Mini-PROTEAN 3 Cell (Bio-Rad) filled with running buffer (25mM Tris, 192mM glycine, 0.1% SDS) and connected to a PowerPac Basic Power Supply (Bio-Rad)

outputting a constant voltage of 150V. Separation was carried out at room temperature and until the front of the run reached the bottom end of the gel. A molecular weight standard (Precision Plus Protein Dual Color Standards, from Bio-Rad) was included to allow molecular weight estimation.

Once protein separation was complete, proteins were transferred to a thin surface layer of pre-activated (5 sec in 100% methanol followed by 15 min in 25mM Tris, 190mM glycine and 20% methanol) 0.45μm polyvinylidene difluoride membrane (PVDF, Millipore, Billerica, MA, USA), by an electric current passed through the gel.

Ponceau S staining was used to ensure equal loading. Once protein transfer was complete the membranes were blocking with 5 % skim milk in TBS-T (50 mM Tris–HCl, pH 8; 154 mM NaCl and 0.1 % Tween-20) or 5% of BSA in TBS-T for 1 h at room temperature or overnight at 4ºC, depending of antibody manufactures description. Then, membranes were incubated overnight at 4 º C with the antibodies (see in Table 1). After three 15 min washes in TBS-T, the membranes were incubated with a dilution (1:5,000 in blocking buffer) of a corresponding alkaline phosphatase-conjugated secondary antibody (Santa Cruz Biotechnology) for 2 h at room temperature. After three 15 min washes in PBS-T, membranes were developed with the ECF detection system (RPN5785; GE Healthcare, Piscataway, NJ) and imaged with Versa Doc imaging system (Bio-Rad) according to the manufacturers' protocols. Densities of each band were calculated with Quantity One Software (Bio-Rad). All data presented are representative from at least three separate experiments.

Table 1 – List of primary antibodies used in Western Blot protein analysis.

Code	Dilution	Host Species	Molecular weight (KDa)	% polyacrilamide	Catalog Number	Manufacturer
AIF	1:1000	Mouse	57	12	sc13116	Santa Cruz
CLS1	1:500	Goat	33.5	14	orb125195	Biorbyt
Taffazin	1:500	Goat	30	14	sc49760	Santa Cruz
TOM20	1:1000	Rabbit	20	12	sc11415	Santa Cruz

3.15 - Lipid peroxidation

Measurement of malondialdehyde (MDA) is a widely used as an indicator of lipid peroxidation. MDA reacts readily with amino groups on proteins and other biomolecules to form a variety of adducts, including cross-linked products.

The levels of MDA were measured by high performance liquid chromatography (HPLC) separation. P19 cells were harvested, washed and re-suspended in 50 mM phosphate buffer (pH 7.4) and stored at -80ºC until used. Then, levels of lipid peroxidation were assessed by the fluorymetric determination (excitation at 515 nm and emission at 553 nm; FP-2020/2025, Jasco, Tokyo, Japan) of MDA adducts separated by HPLC (Gilson; Middleton, WI, USA) using the ClinRep complete kit (RECIPE; Munich, Germany).

3.16 - Cardiolipin peroxidation

In this present work, CL peroxidation was measured using the 10-*N*-nonyl acridine Orange (NAO) fluorescent probe. NAO is able to bind with high affinity to non-oxidized cardiolipin (green-fluorescence). When in the presence of oxidized CL, NAO has been reported to bind with a decrease affinity reflected by lower green fluorescence[87,88,89]. We thus analyzed the loss of the fluorescence peak of NAO that is proportional to an increase of CL peroxidized levels.

For the assay, cells were seeded in 100mm plates at a concentration of $0.5x10^4$ cells/ml for P19 CSCs and $2x10^4$ cells/ml for P19 dCCs. Twenty-four hours after seeding, group of cells were treated with different compounds: H_2O_2 (500 µM) during 4h, melatonin (1 mM) and DCA (10 mM) during 72h. After that, cells were washed, trypsinized and centrifuged at 210g for 10 minutes ate 4°C. The cell pellets were washed in 1ml of PBS and centrifuged again. The resultant cell pellets were re-suspended in 0,1 µM of NAO in PBS, incubated for 30 minutes at 37°C /5% CO_2 in the dark. Then, cells were centrifuged at 210xg for 5 minutes at 4°C and the cell pellet was re-suspended in 0,3ml of PBS and transferred to FACS tubes. The cell suspension (20,000 cells) was analyzed by FACSCalibur flow cytometer (Becton Dickinson, San Jose, California, USA) at low (12 µL/min) sample flow rate. Data was analyzed using BD CellQuest Pro software

package (version 5.2). The fluorescence excitation of NAO were measured at 488nm while the fluorescence emission at 530±15 nm. Two regions were defined, M1 and M2, based on the fluorescence of P19SCs that presented a decrease peroxidized CL and thus, a higher NAO fluorescence. The appearance of a peak in M1 region towards loss of fluorescence in M2 region indicated an increase of CL peroxidation. All the other conditions were compared based on those regions.

3.17 - Isolation of mitochondrial and cytoplasmatic extracts

To collect mitochondrial extracts, P19 cells were harvested by trypsinization and spin down at 1000xg. Pellets were washed once in cold PBS and centrifuged again. The cell suspension was then re-suspended in 0.5ml of ice cold sucrose buffer (250 mM sucrose, 20 mM K^+ Hepes pH 7.5, 10 mM KCl, 1.5 mM $MgCl_2$, 0.1 mM EDTA, 1 mM EGTA) supplemented right before use with 1mM DTT, 0.1mM PMSF and protease inhibitor cocktail containing 1µg/ml of leupeptin, antipain, chymostatin and pepstatin. Then, the suspension was incubated on ice for 20 to 30 minutes. After the incubation, the suspension were transferred to a pre-cooled Potter–Elvehjem homogenizer with a TeXon pestle and homogenized 30 times using a tight pestle, while keeping the homogenizer on ice. The progress was monitored every 20 to 30 strokes under a phase contrast microscope and was stopped when more than 90% of cells were burst.

Homogenized cells were centrifuged at 3500 g for 5 minutes at 4ºC (Evolution RC, Sorvall, USA). The supernatant was collected containing mitochondrial and cytosolic fraction. Then, the supernatant was centrifuged again at 10,000 g during 15 minutes at 4ºC. The pellet, corresponding to the mitochondrial fraction, was re-suspended in 50µl of sucrose buffer cited above. The supernatant was again centrifuged at 100,000xg during 30 minutes at 4ºC (Beckman TL-100 Ultracentrifuge, USA) The resulting supernatant contains the cytosolic fraction and in order to concentrate the protein was lyophilized and re-suspended in 50µl of the same sucrose buffer.

3.18 - Statistical analysis

Data were expressed as mean values ± standard error of mean for a number of independent experiments, specific for each case. Statistical comparisons between P19 CSCs and P19 dCCs were carried out using a Student's t test. The non-parametric test Mann-Whitney was applied to non-normal data. Multiple comparisons were performed using one-way analysis of variance (ANOVA) followed by the Bonferroni post hoc test if the F-values were significant. Significance was accepted with $p<0.05$.

PART 4

RESULTS

4.1- Lipidic profile of P19 cells

Due to the importance of CL, in a variety of pathological settings and its association to the mitochondrial metabolic processes, the study of CL remodeling during cancer stem cells differentiation seems be important. For this reason, we evaluated the lipid profile in undifferentiated and differentiated P19 embryonal carcinoma cells. We also analyzed the lipidic profile when mitochondrial ATP production was forced by growing cells in a galactose, glucose-free, pyruvate/glutamine media.

Phospholipid classes were fractionated by TLC and each class was identified by comparison with applied standards. To evaluate the variation of phospholipid content each spot was quantified using phosphorous assay and the results are shown in figure 4.1.

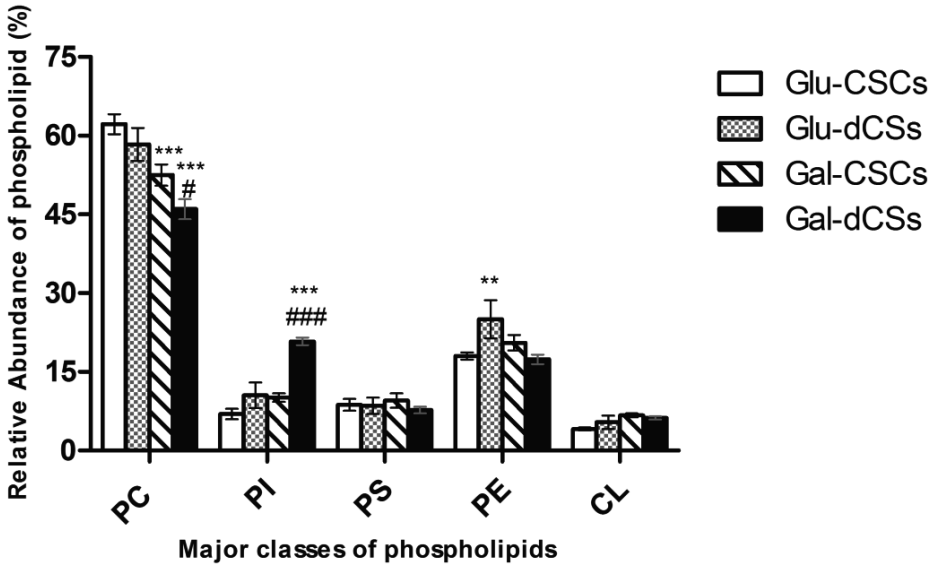

Figure 4.1 - Profile of different phospholipids in P19 EC cells. Phospholipid (PL) content of the four types of P19 cells: stem (CSCs) and differentiated (dCCs) lines, growing in glucose (Glu) and in galactose (Gal)-containing media. PC – phosphatidylcholine, PI – phosphatidylinositol, PS – phosphatidylserine, PE – phosphatidylethanolamine, CL– cardiolipin. Relative abundance of phospholipid refers to the percentage of phospholipid phosphorus recovered from respective TLC. * vs. Glu-CSCs; # vs. Gal-CSCs. Data represent the average percentage of PL content ± SEM from at least five independent experiments The number of symbols denotes statistical significance: one for $p<0.05$, two for $p<0.01$ and three for $p<0.001$.

In all samples, phosphatidylcholine (PC) represented the dominant phospholipid class of total phospholipids followed by phosphatidylethalonamine (PE). Additionally, other phospholipids were also detected with the following order of abundance: phosphatidylserine (PS) > phosphatidylinositol (PI) > CL – in Glu-CSCs; PS/PI > CL – in Gal-CSCs; and PI > PS > CL – in Glu-dCCs and Gal-dCCs. No significant variations between groups were observed for CL content. The content of PC was decreased with the increase in the degree of differentiation being lowest in the P19 cells with the highest differentiation stage, P19 Gal-dCCs. On the contrary, PI levels were statistically increased in cells with maximum mitochondrial activity and highest degree of differentiation (Gal-dCCs). As show the content of CL and PI were lower in Glu-CSCs compared with the others groups of cells. Finally, PE content was only significantly increased in Gu-dCCs in comparison with their undifferentiated counterpart, Glu-CSC ($p < 0.01$).

To complete CL analysis, each spot from P19 Glu-CSCs and Glu-dCCs was studied by mass spectrometry to confirm if the absence of significant changes in the total CL content is also extended to CL molecular species.

4.2– Mass spectrometry analyses for CL species

The characterization of CL molecular species was performed after extraction of silica and analyzed by MS in a negative mode.

CL is located almost exclusively in the mitochondrial inner membrane, is essential for normal mitochondrial energy metabolism and has been implicated in the process of apoptosis. This phospholipid has a dimeric structure, corresponding to two phosphatidylglycerols connected with a glycerol backbone in the center[90]. Cardiolipin has four alkyl groups and potentially possesses two negative charges resulting in either singly charged $[M-H]^-$ or doubly charged $[M-2H]^{2-}$ ions observable in the MS spectra[91]. Singly charged CL ions in negative mode were represented by different molecular clusters with m/z 1373.8, 1401.7, 1403.8, 1425.8, 1427.8, 1449.8, 1455.8, 1451.8, 1479.8, 1501.8 with a variety of fatty acid residues (from C16:0 to C22:6) shown in figure 4.2 The ions formed during fragmentation process of CL (a, b, a+56, or b+136) were identified in MS^2 spectra[91] and are described in Table 1 and shown in figure 4.2,

however in that spectra, only the $[M-H]^-$ fragmentation of clusters with m/z 1401.8; 1427.8; 1455.8; 1449.8; 1479.8 are represented.

The results show evident changes in CL species between both types of P19 cells (Glu-CSCs and Glu-dCCs). The CL species m/z 1427.8 and 1455.8, attributed to the CL $(16:1)(18:2)/(18:1)_2$ and CL $(18:1)_4(18:1)_2(20:2)$ respectively, were highly present in Glu-CSCs; while in Glu-dCCs, CL species with m/z 1427.8 corresponding to CL $(16:1)(18:2)/(18:1)_2$ is the most abundant specie. The relative abundance of the ion m/z 1403.8 attributed to the CL $(16:0)_2(18:1)_2$ had a similar intensities in both types of P19 cells. Overall, Glu-CSCs were enriched with CL species of m/z 1425.8 and 1449.8 corresponding to CL $(16:1)(18:2)(18:1)_2$ and $(18:1)(18:2)_3$ respectively, which were absent in Glu-dCCs. These alterations imply that CL species and fatty acid composition is rather susceptible to the differentiation of P19 stem cells. Therefore, this CL remodeling may have important physiological implications by contributing to the mitochondrial remodeling induced during the differentiation of P19 CSCs.

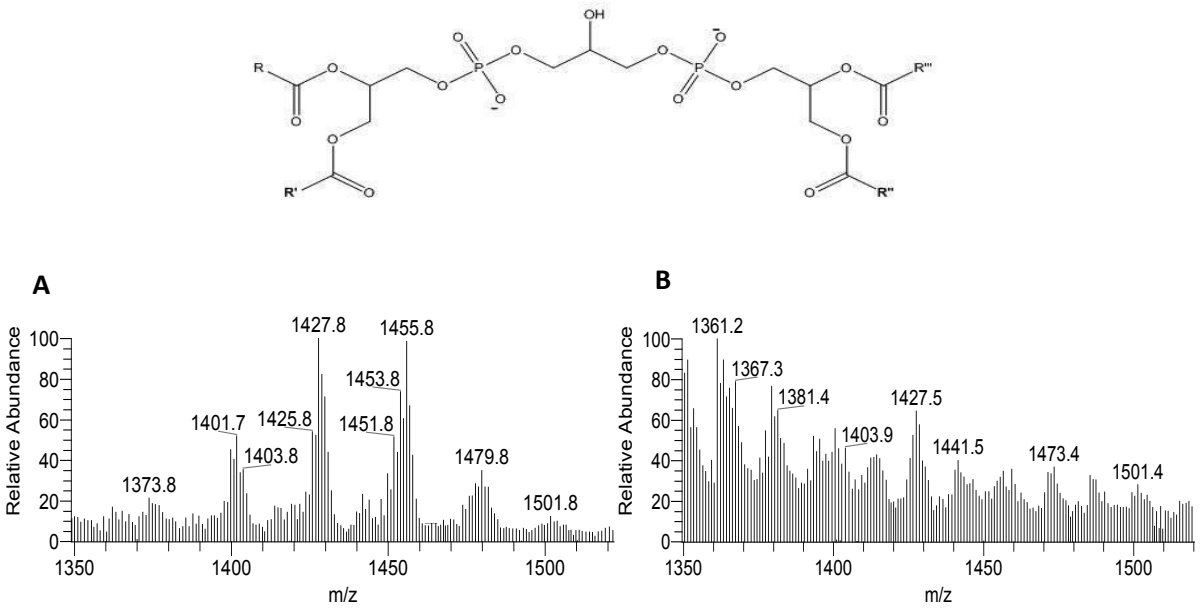

Figure 4.2 - Representative ESI-MS spectrum in negative mode of CL molecular species of P19 Glu-CSCs (**A**) and Glu-dCCs (**B**) and general structure of CL.

Table 2. Major CL molecular species from P19 Glu-CSCs and Glu-dCCs.

CL		Diacyl species
$[M-H]^-$	$[M-2H]^{2-}$	Fatty acyl composition
1401.7	701.5	$(16:0)_2(18:1)(18:2)$
1425.8	712.5	$(16:1)(18:2)(18:1)_2$
1427.8	713.5	$(16:0)(18:1)_2(18:2)$
1449.8	724.5	$(18:1)(18:2)_3$
1451.8	725.5	$(18:1)_2(18:2)_2$
1455.8	727.5	$(18:1)_4(18:1)_2$
1479.8	739.5	$(18:0)(18:1)_2(18:1)_3(20:3)(20:4)$
1501.8	750.5	$(20:4)(20:3)(18:1)_2(22:6)(18:1)_2$

4.3- CL synthesis and remodeling

After general evaluation of CL content and species during the differentiation of P19 EC stem cells we next analyzed the machinery involved in CL synthesis and maturation. For that we measured the content of some proteins associated to those processes including cardiolipin synthase (CLS) and taffazin. CLS is the enzyme that catalyzes the final step in the synthesis of CL from phosphatidylglycerol and CDP-diacylglycerol. Tafazzin is a transmembrane mitochondrial protein that contributing to cardiolipin remodeling modifies and adapts mitochondrial structure and function[59].

Western blot analysis shows a significant increase of CLS1 protein content in differentiated P19 cells (Glu-dCCs and Gal-dCCs) compared their respective stem counterpart (Glu-CSCs and Gal-CSCs). Additionally, higher levels of CLS1 were observed in Gal-dCCs in comparison with the differentiated cells grown in glucose medium.

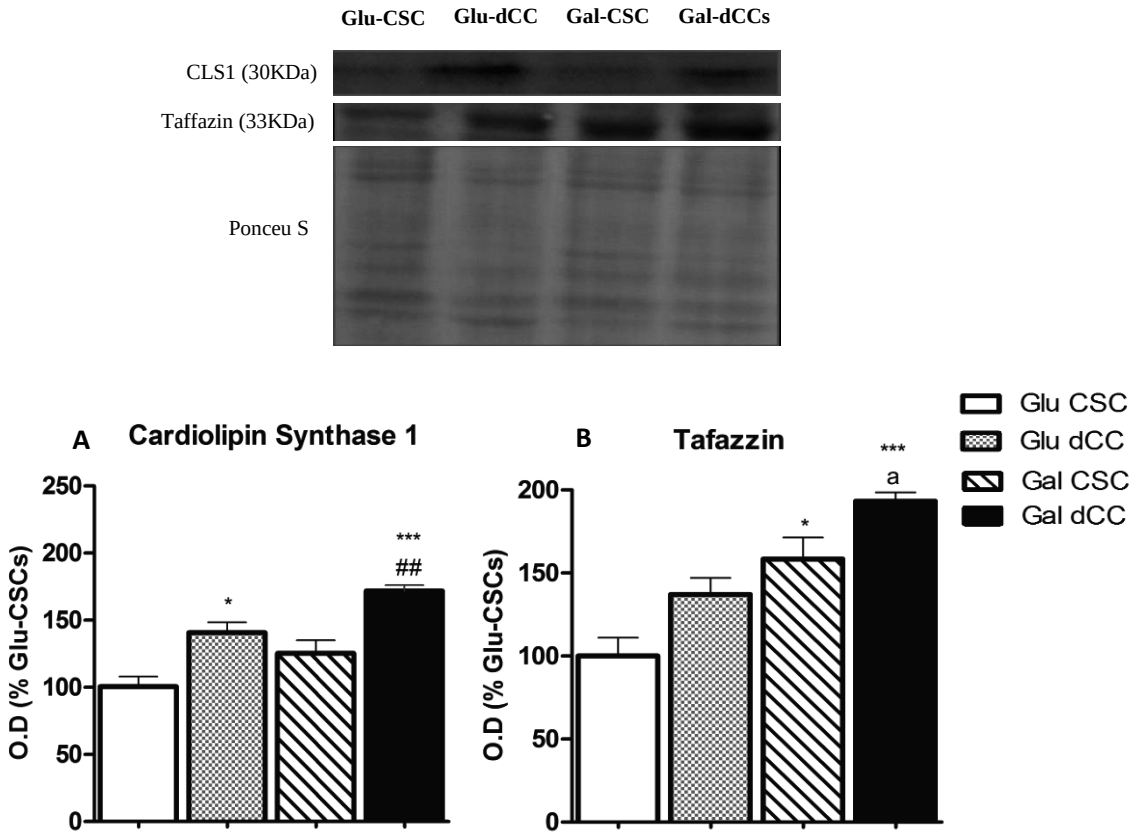

Figure 4.3 - CL synthesis and maturation in the four types of P19 cells. Levels of protein involved in synthesis of CL (CLS1) **(A)** and taffazin **(B),** a protein involved in the formation of mature CL. Bar charts show means of optical density (O.D.) normalized for Ponceu labeling ± S.E.M expressed as percentage of Glu-CSCs, from at least three separate immunoblots. : * vs. Glu-CSCs; # vs. Gal-CSCs; a vs. Glu-dCCs. The number of symbols marks the level of statistical significance: one for $p<0.05$, two for $p<0.01$ and three for $p<0.001$.

In addition, we found higher taffazin content in the P19 cells with higher differentiation degree. Thus, P19 Glu-CSCs presented the lowest content in taffazin. This finding indicates that CL remodeling occurs with cell differentiation being higher in the group of P19 cells with more active mitochondrial metabolism and higher degree of cell differentiation, P19 Gal-dCCs groups.

4.4 – Cardiolipin peroxidation

Apart from analyzing CL biosynthesis and maturation, we also analyzed their oxidation in the four groups of P19 cells. For that, we used the fluorescent NAO probe which has a high affinity for cardiolipin[92].

To evaluate and induce CL peroxidation, we used hydrogen peroxide as a positive control. Hydrogen peroxide has important roles as a signaling molecule in the regulation of a wide variety of biological processes. Hydrogen peroxide can decompose to a hydroxyl radical, a very protect free radical which oxidizes mitochondrial subtracts. For that, we initially verified the toxicity of H_2O_2 in P19 cells using the SRB assay. We tested 500 µM and 1 mM H_2O_2 at different time points (0h, 2h, 4h, and 6h) as previously described[93].

Our results show that all groups of cells were susceptible to H_2O_2. The results showed an increase in the toxic effects of H_2O_2 with cell differentiation (Glu-CSCs – Glu-dCCs – Gal-CSCs – Gal-dCCs). The more undifferentiated cells, Glu-CSCs, presented a more resistant profile against H_2O_2. Taking these results into account, we decided to evaluate CL peroxidation on the four types of P19 cells after 4 h of treatment with 500 µM H_2O_2.

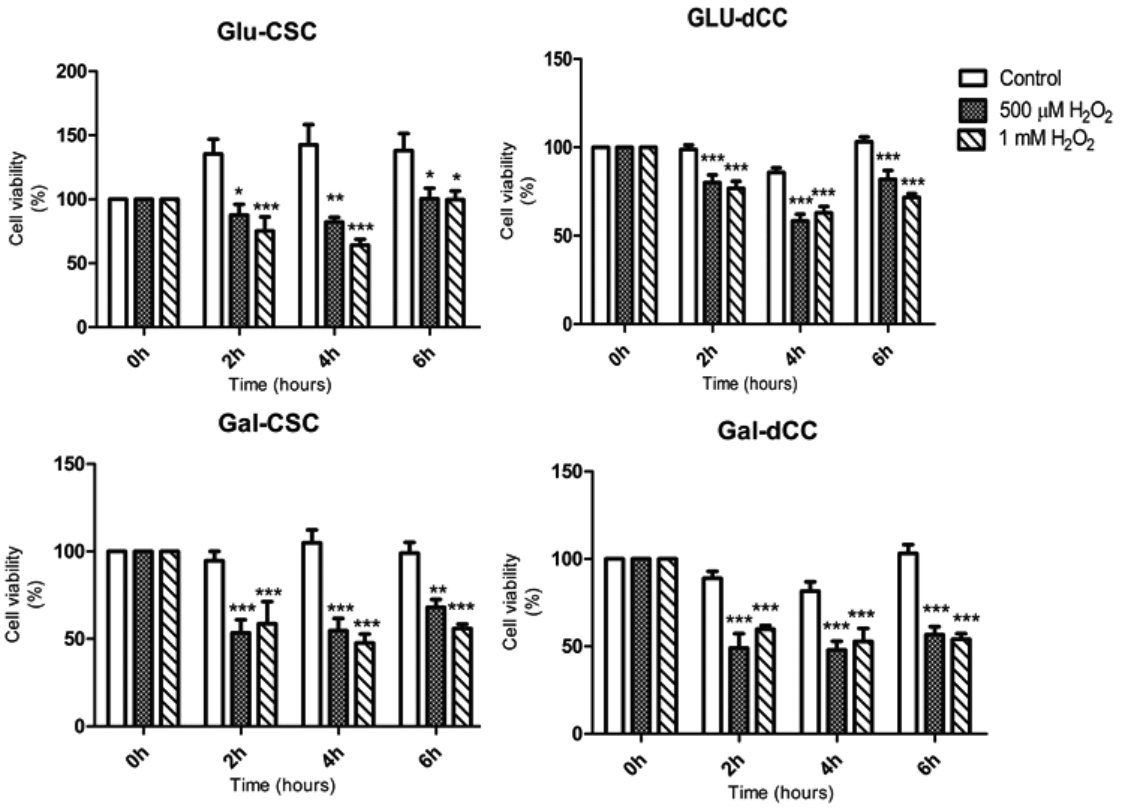

Figura 4.4 - Effect H_2O_2 on cell viability in the four types of P19 cells. Stem (CSCs) and differentiated (dCCs) growing in glucose- (Glu) and galactose-(glucose free) (Gal) containing medium were treated with 500µM and 1mM of H_2O_2 during 2, 4 and 6 hours. Cell viability was measured using the sulforhodamine B cell mass assay. Data are expressed as percentage of the control for time zero. Data are means±S.D rom n±5. *: $p<0.05$; **$p<0.01$; ***: $p<0.001$ versus control.

Cardiolipin has emerged as an essential lipid in controlling the mitochondrial-dependent steps that lead to the release of apoptogenic factors. CL has been described to have an anti-apoptotic function, binding cytochrome c to the mitochondrial inner membrane and thus preventing its release to the intermembrane space[94]. In this scenario, the peroxidation of CL has been shown to lessen the binding of cytochrome c to the inner mitochondrial membrane and facilitate permeabilization of the outer membrane[95]. In this work, we evaluated CL peroxidation in the four different differentiation stages of P19 cells using the NAO specific probe. As shown in figure 4.4A, the loss of NAO fluorescence, what reflects higher CL peroxidation, is shown as a disappearance of the NAO peak signal from region M2 to region M1.

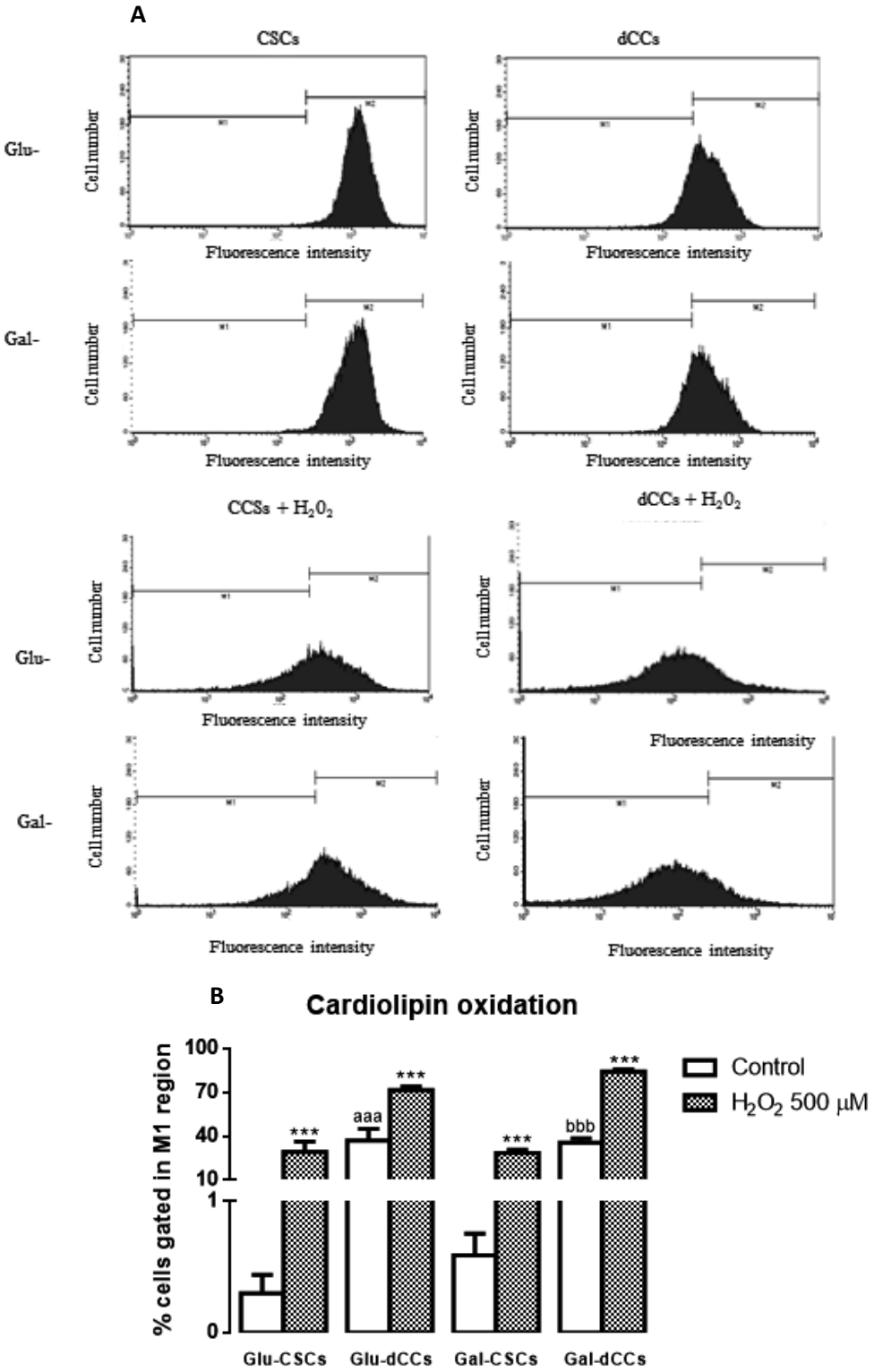

Figure 4.5 - Levels of CL peroxidation in P19 EC cells. The CL peroxidation was monitored by loss of NAO fluorescence measured by flow cytometry. The four group of cells were incubated with 0.1µM of NAO. As positive control, P19 cells were previously incubated for 4h with 500µM of H_2O_2. **(A)** Representative graphics show the loss of NAO fluorescence peak towards the increase of M1 region peak. (**B**) The % cells gated in M1 region indicates the increased of CL oxidation and the results show an increase of CL peroxidation in differentiated cells (Glu-dCCs and Gal-dCCs). Data are means ± S.E.M. from n±6. ***: $p<0.001$ versus control; ^{aaa}: $p<0.001$versus Glu-CSCs and ^{bbb}: $p<0.001$ versus Gal-CSCs.

Our results shown as the percentage of cells with oxidized CL (cells gated on M1 region) revealed evident differences, regardless the culture media used, between stem (Glu-CSCs and Gal-CSCs) and differentiated (Glu-dCCs and Gal-dCCs) P19 cells what might be a consequence of a different mitochondrial redox status generated by the RA-induced mitochondrial remodeling[79]. Thus, Glu-CSCs and Gal-CSCs showed lower levels of peroxidized CL ($p < 0.001$) (Figure 4.5). The treatment with H_2O_2 increased the number of cells in the M1 region in the four groups of P19 cells ($p < 0.001$). However, the effect of H_2O_2 on CL peroxidation was more limited in dCCs probably because their CL is almost oxidized.

4.5 – Melatonin effects on the P19 cancer stem cell model

Melatonin, the main pineal hormone, is known to act as a potent antioxidant by scavenging free radicals and stimulating the activity and expression of antioxidant enzymes. In addition, melatonin has other important roles in mitochondrial activity[77], cell death[81] and presents strong antitumoral properties[83]. The protective effects of melatonin may be produced through its action at mitochondrial level, in which oxidation and/or depletion of CL could play a critical role[96].

To assess the effect of 0.1 and 1 mM melatonin on the four stages of differentiation of P19 cells (Glu-CSCs, Glu-dCCs, Gal-CSCs and Gal-dCCs), we evaluated cell viability using the trypan blue dye assay after 72 hours of treatment. Intriguingly, our results showed that the antiproliferative effect of melatonin was dependent on the culture medium used for cell growth. At 72 hours of incubation, 1 mM melatonin significantly inhibited Gal-CSCs and Gal-dCCs proliferation. Thus, only the cells grown in galactose (glucose free)-containing media which rely in oxidative metabolism for ATP production were sensitive to 1 mM melatonin ($p < 0.01$). Due to this, one can ask what makes these cells prone to melatonin in comparison with the resistant counterparts grown in high glucose medium (Figure 4.6).

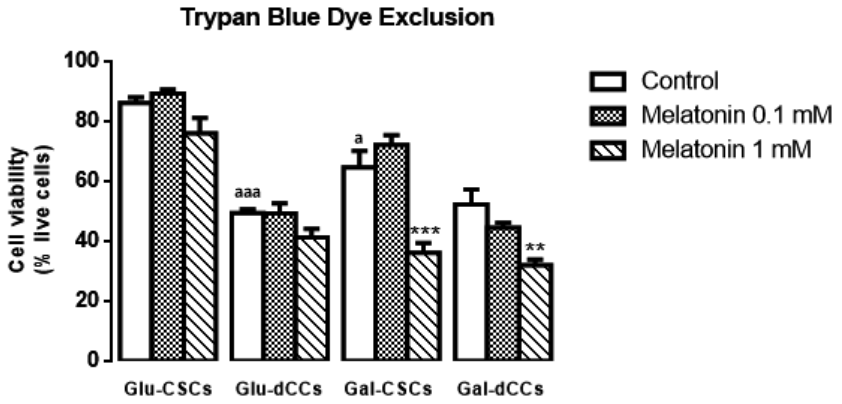

Figure 4.6 - Effects of melatonin in cell viability in P19 EC cells. Cell viability determined by trypan blue dye exclusion assay after 72 hours of treatment with melatonin shows the resistance of P19 cells grown in high glucose medium. Data are expressed as percentage of live cells ± SEM at least three independent experiments. * vs. control; a vs. Glu-CSCs. The number of symbols marks the level of statistical significance: one for $p<0.05$, two for $p<0.01$, and three for $p<0.001$.

The excessive production of ROS can damage all cells components, possibly leading to death pathways. As described, melatonin also presents a pro-oxidant effect in tumor cells as tumor leucocytes[97], lymphoma[98] and hepatic cancinoma[99] cells. Thus, we decided to evaluate the lipidic oxidation as an oxidative stress marker. For that, we measured the content in malondialdehyde (MDA), a ROS-induced lipid peroxidation product.

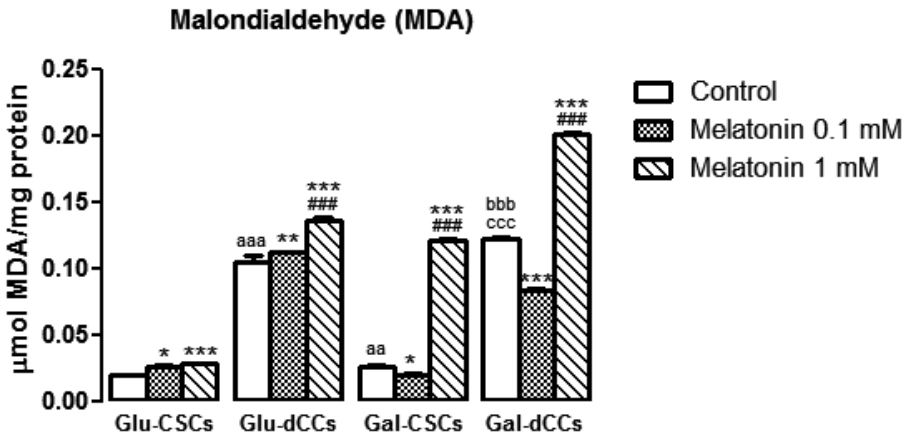

Figure 4.7- Effect of melatonin on lipid peroxidation in the four groups of P19 EC cells. Measurement of malondialdehyde (MDA) by high-performance liquid cromatography in P19 embryonic carcinoma stem (CSCs) and differentiated (dCCs) cells, grown in glucose (Glu) and galatose (Gal) media, after 72 hours of treatment with 0,1 and 1 mM melatonin Statistical comparisons: * vs. control; # vs. 0.1 mM melatonin; a vs. Glu-CSCs; b vs. Gal-CSCs; c vs. Glu-dCCs. The number of symbols marks the level of statistical significance: one for $p<0.05$, two for $p<0.01$ and three for $p<0.001$.

Both groups of P19 differentiated cells (Glu-dCCs and Gal-dCCs) presented a major content of MDA when compared to their stem counterparts ($p < 0.001$) and the cells grown in galactose (Gal-CSCs and Gal-dCCs) also present a higher MDA levels when compared to their glucose-cultured counterpart ($p < 0.01$) (Figure 4.7). Despite these basal differences, we found that 1mM melatonin significantly increased the amount of MDA in all groups of P19 cells when compared to their controls, especially in cells grown in galactose medium ($p < 0.001$) (Figure 4.7). Therefore, this evident prooxidant effect may probably be related to the capacity of melatonin in decreasing the proliferation rate of P19 cells with an active oxidative metabolism. Thus, the prooxidant mechanism of action of melatonin seems to be dependent on the mitochondrial metabolism.

Since excessive ROS production by mitochondria is involved in triggering intrinsic cell death pathways and melatonin increase the lipid-peroxidation in in P19 cells with higher mitochondrial metabolism, we looked to the effect of melatonin in CL peroxidation.

Glu-CSCs presented a resistant profile against melatonin which seems to be closely associated to their glycolytic metabolism. As recently described by our group, there is also a resistant profile of Glu-CSCs against DCA, an anticancer drug that reverses the abnormal metabolism of cancer cells by shifting it from glycolysis to glucose oxidation[79]. As melatonin appears to affect only cells relying on mitochondrial metabolism we wondered if a combined treatment with DCA could make Glu-CSCs prone to melatonin decreasing its proliferation rate. In previously results of our lab we saw a susceptibility in Glu-CSCs to the combined treatment and also a synergetic effect in both types of P19 cells growing in galactose medium (Appendix 3). So, we wanted to verify, in all groups of P19 cells, how melatonin treatment affects the state of CL oxidation using the combined treatment.

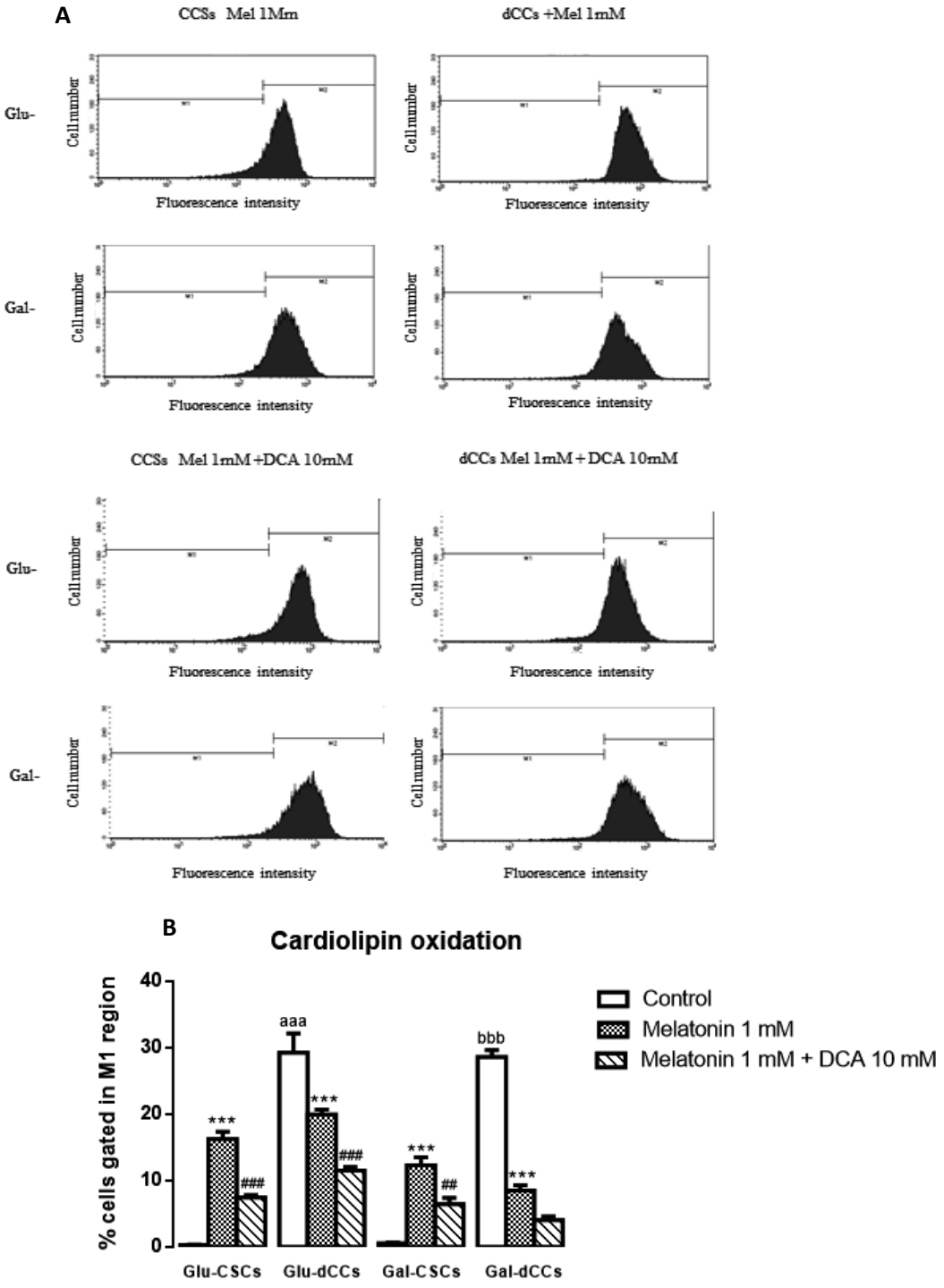

Figure 4.8 - Effects of melatonin on cardiolipin peroxidation. The four group of cells (P19SCs growing and in glucose and galactose (glucose-free) and their differentiated counterparts) were treated during 72h with 1mM melatonin, alone or in combination with10 mM DCA and CL peroxidation was monitored by following the loss of NAO fluorescence by flow cytometry. (**A**) Demonstrative histograms show the loss of NAO fluorescence peak towards the increase of M1 region peak. (**B**) The % cells gated in M1 region indicates increased of CL oxidation. Data are means ± S.E.M. from n±6: * vs. control; # vs. 1 mM melatonin; a vs. Glu-CSCs; b vs. Gal-CSCs. The number of symbols marks the level of statistical significance: one for $p<0.05$, two for $p<0.01$ and three for $p<0.001$.

Figure 4.8 revealed the treatment with melatonin increased the peroxidized CL in CSCs ($p<0,001$) and the opposite effect in dCCs independently of the culture media. These results are shown in the spectra of figure 4.8A with the decreased of NAO fluorescence peak in CSCs. Additionally, the combined treatment with melatonin and DCA had the same effect in CL peroxidation in CSCs and in differentiated cells comparatively of the effect of treatment with melatonin. Thus, melatonin seems prevent the CL oxidation in CSCs and so it may not involve in the antiproliferative effects of melatonin observed in this type of cells.

In addition to the effects of melatonin on CL peroxidation in P19 cells growing in galactose media, previously results of our laboratory showed an absence of caspase-3 activity and translocations of cytochrome c to the cytoplasm in these cells. Thus, the possible cytotoxic mechanisms of melatonin are through of caspases-independent pathway. Independently of caspase activation, cell death can occur with the release of endonuclease G (Endo G) and apoptosis inducing-factor (AIF). The basic mechanism of AIF-induced cell death consists in its release from the mitochondrial intermembrane space to the cytosol and translocation to the nucleus.

In this work we proposed to verify if the release of the AIF from mitochondria is involved in the cytotoxic effect elicited by melatonin in P19 cells. For that, we checked the protein content of AIF by western blotting, in mitochondrial and cytosolic fractions from P19 cells treated with 1 mM melatonin alone or in combination with 10 mM DCA.

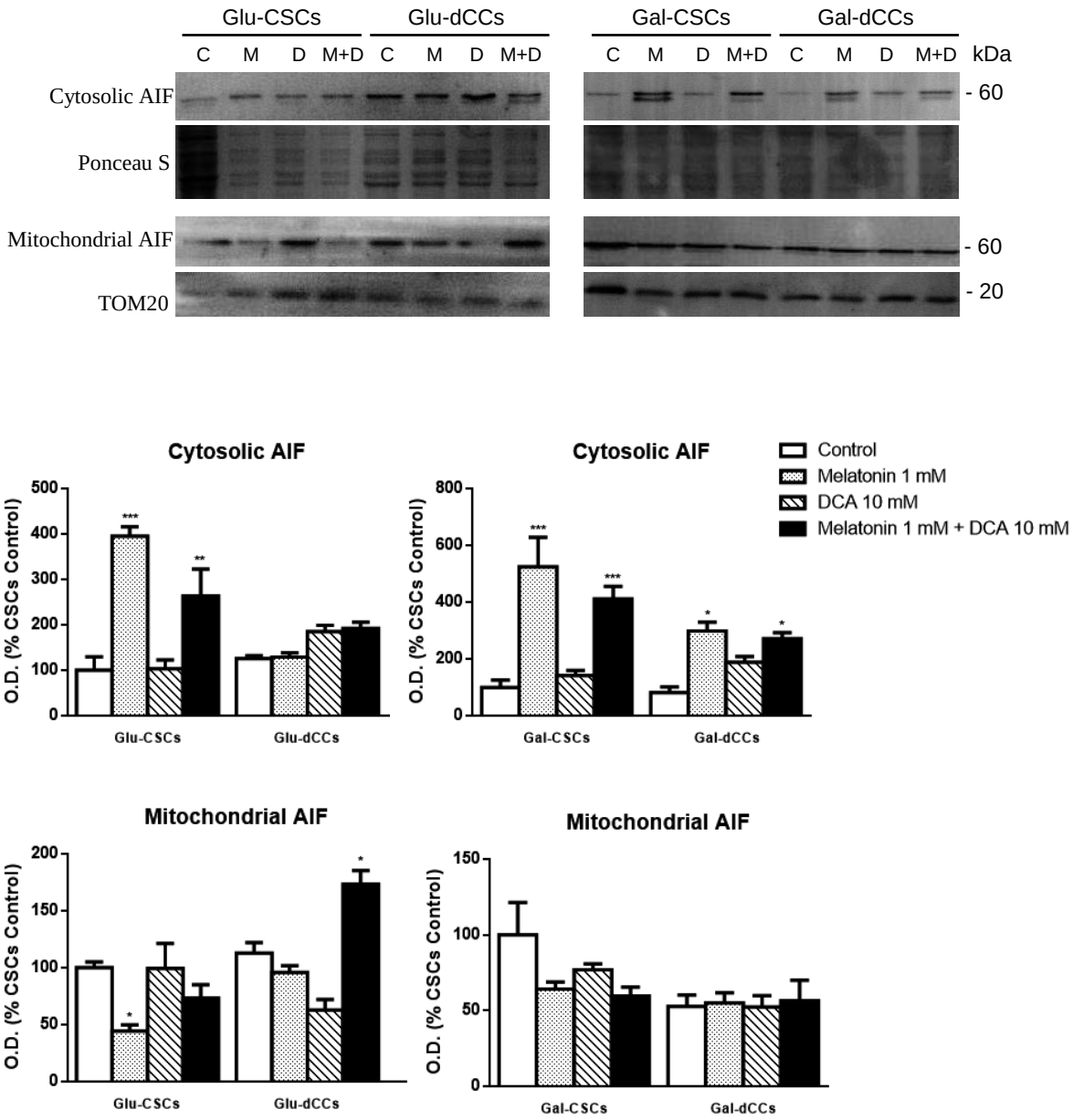

Figure 4.9 - Cytotoxic effects of melatonin in P19 cells. Representative immunoblot images for apoptosis-inducing factor (AIF) in cytosolic and mitochondrial extracts from P19 stem (CSCs) and differentiated (dCCs) cells, grown in glucose (Glu) and galatose (Gal) media. Treatments: control (C), melatonin 1 mM (M), dichloroacetate 10 mM (D), and melatonin 1 mM + dichloroacetate 10 mM (M+D). Ponceau S was used as cytosolic loading control and TOM20 as a mitochondrial loading control. Bar charts show means of normalized optical density (O.D.) ± SEM expressed as percentage of CSCs control, from at least three separate immunoblots. Statistical comparisons: * $p<0.05$; ** $p<0.01$; *** $p<0.001$ vs. control.

The immunoblot analysis revealed that the treatment with melatonin, alone or in combination with dichloroacetate, induces a higher cytosolic localization of AIF in both types of P19 cells grown in galactose medium. In addition, although the treatments with melatonin also increased the cytosolic expression of AIF in the highly resistant Glu-CSCs, in melatonin-treated cells grown in galactose medium (Gal-CSCs and Gal-dCCs) and in Glu-dCCs treated with melatonin and DCA, we observed an additional cytosolic band of ~57 kDa which probably corresponds to the form of AIF described to be translocated to the nucleus triggering a caspase-independent type of cell death (Figure 4.9).

PART 5

DISCUSSION

Due to the relation of CL with mitochondrial apoptosis, an analysis in CSCs under different stages of differentiation would help to elucidate the mechanisms of CSCs resistance to mitochondrial targeted-therapies. In this study we compare the remodeling of mitochondrial CL during P19 CSCs differentiation.

CL provides a paradigmatic example for the role of phospholipids in mitochondrial structure and function. Recent evidences demonstrated similar mitochondrial mass and mtDNA copy number between P19 stem and differentiated cells[47,48,79]. In fact, our results demonstrated no significant changes in total CL levels after the differentiation induced by the treatment with retinoic acid. However, it is possible to see that P19 cells with a more active mitochondrial metabolism present a small increase in total CL. These evidences probably result of the increase in the expression of mitochondrial respiratory complexes, previously described[79], which require CL for their assembly in mitochondrial membrane. Furthermore, CL form hexagonal phases that can create tension in membranes which have functional importance to various mitochondrial processes such as membrane fusion or the movement of proteins or solutes across membranes[100]. Thus, it is likely that more CL seems be required for the differentiation of P19 cells. In agreement with our results, other studies already described, minor changes in CL content in carcinoma[101] and stem cells[102] differentiation, which was in some cases associated to increased mitochondrial activity during this process.

Although we have not found statistical differences in total CL content after the RA-induced differentiation, we observed several alterations regarding CL species in P19 EC cells grown in glucose medium. In fact, P19 Glu-CSCs possessed a higher incorporation of oleic acid (18:1) compared with its differentiated counterpart. This evidence suggests that a higher content in non-oxidized CL may protect these cells against apoptosis, caused by anti-cancer agents, as previously described[103]. Contrarily, Glu-dCCs have more of palmitoleic and linoleic acids and peroxidized CL which probably make these cells more susceptible to apoptosis than Glu-CSCs. In fact, during early stages of intrinsic apoptosis, the CL/cytochrome c complexes exhibit a potent peroxidase activity and the polyunsaturated species of CL have been identified as a preferential oxidation substrate for cytochrome c in vitro[104,105] and also in vivo[106,107]. Thus, the accumulation of CL oxidation products in mitochondria of apoptotic cells has been found to be essential for the release of pro-apoptotic factors into the cytosol[103,108]. It was recently described that an integration of mono-unsaturated oleic acid into mitochondrial CL in mouse embryonic cells, led to the desensitization of apoptosis via suppression of CL

oxidation[103]. Furthermore, the inhibition of long chain acyl-CoA synthase reinstated polyunsaturation of CL and sensitivity to apoptosis [103].

Several studies have suggested a closed relationship between mitochondrial function and lipid composition. PC and PE are the most abundant phospholipids. Each class of phospholipid presents a unique molecular profile which independently of fatty acid composition modulates membrane structure[109]. Our results demonstrated lower levels of PC in P19 cells with forced oxidative metabolism which has been described during the differentiation of carcinoma embryonic cell line[102]. The increase of OXPHOS activity present in P19 cells growing in galactose-modified medium and consequent increased expression of some components of mitochondrial respiratory complexes, as complex II and IV subunits[79] may result in a recruitment of several proteins to mitochondria. That protein translocation probably cause of transfer of PC between subcellular compartments and interaction with proteins. Thus, a loss of PC levels was detectable, as previously described during the differentiation of P19 cells into cardomiocytes[111] and in a breast cancer cell line[112]. Differences in PE levels were also observed in P19 cells. PE is known to increase activity of cytochrome c oxidase, oxygen consumption and also the mitochondrial membrane potential[113]. In fact, we observed in P19 differentiated cells growing in glucose media increased mitochondrial membrane potential as well as increased oxygen consumption compared with their stemness counterparts[79]. Thus, increased of PE in Glu-dCCs may suggest its requirement for all of the processes associated with cell differentiation. However, when mitochondrial metabolism was forced the PE levels did not follow the tendency of Glu-dCCs, which may be related with some impairment in PE biosynthesis or loss of detectable PE in Gal-P19cells.

Although significantly changes were not observed in the content of total CL during the differentiation of P19 cells with RA, CL synthesis and remodeling may be increased, with increased CL oxidation being observed. These findings suggest that P19 cells differentiation with RA increases the mitochondria activity and may allow the synthesis and translocation of mitochondrial enzymes for the processes of synthesis and remodeling of CL. The higher content of CLS in P19 dCCs seems to be a consequence of the higher mitochondrial activity and biogenesis promoted by the RA- induced cell differentiation[79]. Furthermore, we found that the content of taffazin increased in the cells with higher active mitochondrial metabolism. All these results support our hypothesis and previous findings about the strong mitochondrial remodeling induced during the differentiation of CSCs at both structural and functional levels[79]. As

previously observed, a stronger expression of taffazin is associated with primary rectal cancer development and metastasis compared to distant or adjacent normal mucosa[114]. Furthermore, it is interesting notice that decreased the taffazin content is observed after anti-cancer therapy[114]. However our results showed higher content of taffazin in P19 cells with higher mitochondrial activity, cells which are more susceptible to death. Thus, the remodeling of CL, by the presence of higher contents of taffazin, must be a reason for susceptibility in cells with active mitochondrial metabolism. Moreover, alterations in taffazin content may lead to different molecular species of CL observed during the differentiation of P19 EC cells as also described during differentiation of embryonic stem cells into cardiomyocytes, where the depletion of taffazin altered the pattern of molecular species of CL and also increased mitochondria with abnormal cristae[115].

The role of CL in mitochondrial activity and structure as well as in apoptosis was extensively investigated. It is known that the decline in mitochondrial respiratory functions leads to the accumulation of ROS. Under normal physiological conditions mitochondrial CL may protect cells from oxidative stress through the deacylation-reacylation cycle[116]. However, CL is also a vulnerable target of ROS due to its unsaturated acyl chains and its close proximity to ROS generation sites[116]. It is also clear that during many cell death processes ROS and loss of CL are closely linked in a cycle of CL peroxidation. Recently evidences described that during P19 differentiation, higher content of mitochondrial superoxide anion is formed providing further evidence of mitochondrial remodeling during differentiation[79]. In this work we found an increase of peroxidized CL in differentiated cells (Glu-dCC and Gal-dCCs) in comparison to their stem counterparts which agree with the higher levels of ROS previously found in this type of P19 cells. The presence of peroxidized CL during apoptosis is usually described[107,130] since this state of CL leads to its dissociation to cytochrome c allowing its release form mitochondria triggering the subsequent apoptotic events[61]. Thus, the more susceptible to mitochondrial poisons observed in P19 differentiated cells[79] may be correlated with the higher CL peroxidation.

In this work, we also evaluated the susceptibility of the four types of P19 cells studied to the main pineal hormone melatonin which have showed effective protective actions against several pathologic states through the impact on CL peroxidation[96]. Besides being a natural and potent free radical scavenger[78,83], melatonin is reported to inhibits CL peroxidation in mitochondria preventing mitochondrial permeability transition and

cytochrome c release[116], and therefore, regulating apoptosis[117]. In this work, we demonstrated that melatonin was not effective in reducing cell proliferation in P19 cells grown in high glucose medium. Interestingly, only cells grown in galactose-(glucose-free) and glutamine-containing media were susceptible to the indolamine. Resistance to therapy, a hallmark of CSCs, seems to be strongly linked with the metabolic profile. Thus, some tumor cells are unable to produce ATP through mitochondria establishing a mitochondrial apoptosis resistant profile[118]. This glycolytic metabolism is also characteristic of many normal stem cells[119]. Moreover, melatonin induced a prooxidant effect increasing lipid peroxidation in the P19 cells with an active oxidative metabolism. Thus, this prooxidant effect of melatonin may be related to its ability in decreasing the proliferation rate of some types of cancer cells[97]. Our results suggest that melatonin exerts its antiproliferative actions only in those cells which rely predominantly on oxidative phosphorylation for ATP synthesis by an action mediated by an increase in ROS production.

A resistant profile of P19 Glu-CSCs against DCA, an anticancer drug that reverses the abnormal metabolism of cancer cells by shifting it from glycolysis to glucose oxidation was recently described[79]. In fact, just RA-induced P19 differentiated cells are susceptible to the effects of DCA, and its effects were higher with the increased of DCA concentration[79]. Thus, here we tested if the combination of melatonin with DCA could decrease the proliferation rate of P19 CSCs. In fact, we confirmed that the combined treatment decreases cell viability in all types of P19 cells (Appendix 3). Moreover, Glu-CSCs resistant to the treatment with melatonin and DCA separately became susceptible when applied the combined treatment. After these evidences, we wanted to verify if the effect of the combined treatment was a consequence of higher CL peroxidation. We observed less peroxidized CL in RA differentiated cells treated with melatonin. In addition, the same effect was observed with the conjugated treatment. Hence, we may conclude that melatonin is able to prevent CL peroxidation in P19 differentiated cells as previously described[96], and that the peroxidation of CL may not be the mechanism through which melatonin inhibits proliferation of both types of P19 cells with active mitochondrial metabolism (Gal-CSCs and Gal-dCCs). Taking into account all our results in the P19 cell line, we can infer that melatonin probably induces its cytotoxic effect via the inhibition of mitochondrial metabolism as also described in other types of tumor cells[120]. P19 Glu-CSCs present a strong resistant phenotype which seems to be extremely linked with their glycolytic metabolism. In fact, our group previously found

that only P19 cells with an active mitochondrial metabolism are susceptible to the anticancer agent DCA[8]. Furthermore, our results suggest that melatonin exert its cytotoxic effects also in P19 cells with an active oxidative metabolism, triggering a type of mitochondrial cell death which is caspases independent and which may involve the AIF. A similar pathway of melatonin-induced apoptosis was also observed in other types of cancer cells like MCF-7[121]. Therefore, mitochondrial activity, function and differentiation strongly impact the antitumoral hability of melatonin which involves, among others, the activation of intrinsic apoptotic pathways, at least in P19 embryonal carcinoma cells and in other types of cancer cells[120]. It is known that AIF controls programmed cell death during early morphogenesis and that genetic inactivation of AIF renders embryonic stem cells resistant to cell death[122]. Thus, the mechanism of caspase-independent cell death and the stimulation of mitochondrial metabolism constitute promissory strategies when targeting resistant cancer cells with an embryonic signature like P19 CSCs. In this context, these results support the possible use of melatonin-based treatments in limiting CSCs growth.

Hence, CL undergoes an intense remodeling during P19 CSCs differentiation that probably contributes in turning these cells susceptible to mitochondrial-targeted antitumor agents, while possibly participating in metabolic remodeling.

PART 6

CONCLUSIONS

Cardiolipin is emerging as an important factor in the regulation of several mitochondrial processes, including respiratory chain complexes activity, inner membrane supermolecular assembly, anion carrier activity, binding of cytochrome c and functioning of other multiple mitochondrial inner membrane enzymes. Cardiolipin is also emerging as an important player in the control of mitochondrial apoptosis.
In this thesis we can conclude that:

- Cardiolipin remodeling accompanies the metabolic transformation towards a more oxidative metabolism that occurs during the differentiation of P19 CSCs.
- The differentiation of P19 CSCs also induces the peroxidation of cardiolipin. The incorporation of oleic acid into cardiolipin from P19 CSCs allows us to conclude that P19 CSCs present a lower amount of non-oxidized cardiolipin.
- Melatonin is only effective in reducing proliferation of P19 cells with higher oxidative metabolism. Furthermore, melatonin is able to prevent cardiolipin peroxidation only in the P19 cells with more peroxidized cardiolipin (dCCs). In P19 CSCs, melatonin induces cardiolipin peroxidation. However, this mechanism is not the main contributor for melatonin antiproliferative actions in this cellular model.
- The cytotoxic effects of melatonin in these cells with active oxidative metabolism could be mediated by triggering a type of mitochondrial cell death which may be mediated by AIF.

PART 7

FUTURE PERSPECTIVES

Regarding all the results present in this work and given the critical importance to cardiolipin, a mitochondrial phospholipid, as having a high potential in the regulation of the apoptosis, we plan to investigate the mechanisms underlying CL regulation in differentiation of P19 ESC. Moreover, we plan in assessing how CL will bring value information about the chemotherapies resistance in this CSCs model.

To further explore these mechanisms, we propose silencing CLS in these cells. First, we will confirm the effects of CLS silencing in P19 differentiation, trough the expression of differentiation markers such as Musashi, betaIII-tubulin and TROMA1. Then, we plan verify the CL content and peroxidation using the TLC and NAO probe respectively. After this we will check the phenotype resulting from CLS silencing on differentiation through the oxygen consumption and the transmembrane potential in P19 cells in different stages of differentiation

Regarding the role of CL in resistance to chemotherapeutics, we proposed evaluate CLS silencing effects in cell susceptibility to chemotherapies. In addition to the compounds already used in this work (DCA and melatonin) we plan to use doxorubicin and etoposidium described as effective antitumor agents[123,124,125]. Furthermore, we plan to identify the apoptotic events associated with the treatment with these four agents, measuring the release of cytochrome c from mitochondria to the cytoplasmatic region, measure caspases 3 and 9 activities and finally induction of the mitochondrial permeability transition.

Finally, to consolidate the results obtained in this work, we also propose evaluate the expression of CLS and taffazin in cells treated with DCA and melatonin in concentrations previously administrated, and thus verify whether these two agents affect the synthesis and remodeling of CL.

PART 8

BIBLIOGRAPHY

1- Soltysova, A., Altanerova, V., Altaner, C. (2005). "Cancer stem cells." Neoplasma **52**(6): 435-440.

2- Frankel, M. S. (2000). "In search of stem cell policy." Science **287**(5457): 1397.

3- Reya, T., Morrison, S. J., Clarke, M. F., Weissman, I. L. (2001). "Stem cells, cancer, and cancer stem cells." Nature **414**(6859): 105-111.

4- Eyler, C. E. and J. N. Rich (2008). "Survival of the fittest: cancer stem cells in therapeutic resistance and angiogenesis." J Clin Oncol **26**(17): 2839-2845.

5- Campbell, L. L. and K. Polyak (2007). "Breast tumor heterogeneity: cancer stem cells or clonal evolution?" Cell Cycle **6**(19): 2332-2338.

6- Damjanov, I. (2004). "From stem cells to germ cell tumors and back." Verh Dtsch Ges Pathol **88**: 39-44.

7- Nicolas, J. F., Dubois, P., Jakob, H., Gaillard, J., Jacob, F. (1975). "[Mouse teratocarcinoma: differentiation in cultures of a multipotential primitive cell line (author's transl)]." Ann Microbiol (Paris) **126**(1): 3-22.

8- Martin.G.R. and Evans,M.J.(1975). Multiple differentiation of clonal teratocarcinoma stem cells following embryoid body formation in *vitro.* Cell (6): 467-474.

9- Jones-Villeneuve, E. M., McBurney, M. W., Rogers, K. A., Kalnins, V. I. (1982). "Retinoic acid induces embryonal carcinoma cells to differentiate into neurons and glial cells." J Cell Biol **94**(2): 253-262.

10- McBurney, M. W., Jones-Villeneuve, E. M., Edwards, M. K., Anderson, P. J. (1982). "Control of muscle and neuronal differentiation in a cultured embryonal carcinoma cell line." Nature **299**(5879): 165-167.

11- Edwards, M. K., Harris, J. F., McBurney, M. W. (1983). "Induced muscle differentiation in an embryonal carcinoma cell line." Mol Cell Biol **3**(12): 2280-2286.

12- Schubert, D., Kimura, H., LaCorbiere, M., Vaughan, J., Karr, D., Fischer, W. H.. (1990). "Activin is a nerve cell survival molecule." Nature **344**(6269): 868-870.

13- McBurney, M. W. (1993). "P19 embryonal carcinoma cells." Int J Dev Biol **37**(1): 135-140.

14- Evans, R. M. (1988). "The steroid and thyroid hormone receptor superfamily." Science **240**(4854): 889-895

15- Marshall, H., Morrison, A., Studer, M., Popperl, H., Krumlauf, R. (1996). "Retinoids and Hox genes." FASEB J **10**(9): 969-978.

16- Duester, G. (2008). "Retinoic acid synthesis and signaling during early organogenesis." Cell **134**(6): 921-931.

17- Jones-Villeneuve, E. M., Rudnicki, M. A., Harris, J. F., McBurney, M. W. (1983). "Retinoic acid-induced neural differentiation of embryonal carcinoma cells." Mol Cell Biol **3**(12): 2271-2279.

18- Morley, P. and J. F. Whitfield (1993). "The differentiation inducer, dimethyl sulfoxide, transiently increases the intracellular calcium ion concentration in various cell types." J Cell Physiol **156**(2): 219-225.

19- Dean, M., Fojo, T., Bates, S. (2005). "Tumour stem cells and drug resistance." Nat Rev Cancer **5**(4): 275-284.

20- Gottesman, M. M., Fojo, T., Bates, S. E. (2002). "Multidrug resistance in cancer: role of ATP-dependent transporters." Nat Rev Cancer **2**(1): 48-58.

21- Viale, A., De Franco, F., Orleth, A., Cambiaghi, V., Giuliani, V., Bossi, D., Ronchini, C., Ronzoni, S., Muradore, I., Monestiroli, S., Gobbi, A., Alcalay, M., Minucci, S., Pelicci, P. G. (2009). "Cell-cycle restriction limits DNA damage and maintains self-renewal of leukaemia stem cells." Nature **457**(7225): 51-56.

22- Schatton, T., Murphy, G. F., Frank, N. Y., Yamaura, K., Waaga-Gasser, A. M., Gasser, M., Zhan, Q., Jordan, S., Duncan, L. M., Weishaupt, C., Fuhlbrigge, R. C., Kupper, T. S., Sayegh, M. H., Frank, M. H. (2008). "Identification of cells initiating human melanomas." Nature **451**(7176): 345-349.

23- Frank, N. Y., Margaryan, A., Huang, Y., Schatton, T., Waaga-Gasser, A. M., Gasser, M., Sayegh, M. H., Sadee, W., Frank, M. H. (2005). "ABCB5-mediated doxorubicin transport and chemoresistance in human malignant melanoma." Cancer Res **65**(10): 4320-4333.

24- Li, X., Lewis, M. T., Huang, J., Gutierrez, C., Osborne, C. K., Wu, M. F., Hilsenbeck, S., Pavlick, A., Zhang, X., Chamness, G. C., Wong, H., Rosen, J., Chang, J. C. (2008). "Intrinsic resistance of tumorigenic breast cancer cells to chemotherapy." J Natl Cancer Inst **100**(9): 672-679.

25- Bao, S., Wu, Q., McLendon, R. E., Hao, Y., Shi, Q., Hjelmeland, A. B., Dewhirst, M. W., Bigner, D. D., Rich, J. N.. (2006). "Glioma stem cells promote radioresistance by preferential activation of the DNA damage response." Nature **444**(7120): 756-760.

26- Diehn, M., Cho, R. W., Lobo, N. A., Kalisky, T., Dorie, M. J., Kulp, A. N., Qian, D., Lam, J. S., Ailles, L. E., Wong, M., Joshua, B., Kaplan, M. J., Wapnir, I., Dirbas, F. M., Somlo, G., Garberoglio, C., Paz, B., Shen, J., Lau, S. K., Quake, S. R., Brown, J. M., Weissman, I. L., Clarke, M. F. (2009). "Association of reactive oxygen species levels and radioresistance in cancer stem cells." Nature **458**(7239): 780-783.

27- Kroemer, G. (1999). "Mitochondrial control of apoptosis: an overview." Biochem Soc Symp **66**: 1-15.

28- Pommier, Y., Sordet, O., Antony, S., Hayward, R. L., Kohn, K. W. (2004). "Apoptosis defects and chemotherapy resistance: molecular interaction maps and networks." Oncogene **23**(16): 2934-2949.

29- Zhang, L., Yu, J., Park, B. H., Kinzler, K. W., Vogelstein, B.. (2000). "Role of BAX in the apoptotic response to anticancer agents." Science **290**(5493): 989-992

30- Schott, A. F., Apel, I. J., Nunez, G., Clarke, M. F. (1995). "Bcl-XL protects cancer cells from p53-mediated apoptosis." Oncogene **11**(7): 1389-1394.

31- Gomes, C. M., van Paassen, H., Romeo, S., Welling, M. M., Feitsma, R. I., Abrunhosa, A. J., Botelho, M. F., Hogendoorn, P. C., Pauwels, E., Cleton-Jansen, A. M. (2006). "Multidrug resistance mediated by ABC transporters in osteosarcoma cell lines: mRNA analysis and functional radiotracer studies." Nucl Med Biol **33**(7): 831-840.

32- Burger, H., et al. (1994). "Expression of the multidrug resistance-associated protein (MRP) in acute and chronic leukemias." Leukemia **8**(6): 990-997.

33- Minderman, H., et al. (2004). "VX-710 (biricodar) increases drug retention and enhances chemosensitivity in resistant cells overexpressing P-glycoprotein, multidrug resistance protein, and breast cancer resistance protein." Clin Cancer Res **10**(5): 1826-1834.

34- Stavrovskaya, A. A. (2000). "Cellular mechanisms of multidrug resistance of tumor cells." Biochemistry (Mosc) **65**(1): 95-106.

35- Hadnagy, A., Gaboury, L., Beaulieu, R., Balicki, D. (2006). "SP analysis may be used to identify cancer stem cell populations." Exp Cell Res **312**(19): 3701-3710.

36- Luqmani, Y. A. (2005). "Mechanisms of drug resistance in cancer chemotherapy." Med Princ Pract **14 Suppl 1**: 35-48.

37- Bertolini, G., et al. (2009). "Highly tumorigenic lung cancer CD133+ cells display stem-like features and are spared by cisplatin treatment." Proc Natl Acad Sci U S A **106**(38): 16281-16286.

38- Visvader, J. E. and G. J. Lindeman (2008). "Cancer stem cells in solid tumours: accumulating evidence and unresolved questions." Nat Rev Cancer **8**(10): 755-768.

39- Munz, M., et al. (2010). "Side-by-side analysis of five clinically tested anti-EpCAM monoclonal antibodies." Cancer Cell Int **10**: 44.

40- Brischwein, K., et al. (2006). "MT110: a novel bispecific single-chain antibody construct with high efficacy in eradicating established tumors." Mol Immunol **43**(8): 1129-1143.

41- Schatton, T., et al. (2008). "Identification of cells initiating human melanomas." Nature **451**(7176): 345-349.

42- Lonergan, T., et al. (2007). "Mitochondria in stem cells." Mitochondrion **7**(5): 289-296.

43- McBride, H. M., Neuspiel, M., Wasiak, S. (2006). "Mitochondria: more than just a powerhouse." Curr Biol **16**(14): R551-560.

44- Pedersen, P. L. (1978). "Tumor mitochondria and the bioenergetics of cancer cells." Prog Exp Tumor Res **22**: 190-274

45- Warburg, O. (1956). "On the origin of cancer cells." Science **123**(3191): 309-314.

46- Rodrıguez-Enrıquez, S., Juarez, O., Rodrıguez-Zavala, J. S., Moreno-Sanchez, R. (2001). Multisite control of the Crabtree effect in ascites hepatoma cells. Eur. J. Biochem. 268, 2512–2519.

47- Watkins, J., Basu, S., Bogenhagen, D. F. (2008). "A quantitative proteomic analysis of mitochondrial participation in p19 cell neuronal differentiation." J Proteome Res **7**(1): 328-338.

48- Singh, G. and K. L. Veltri (1991). "Effects of differentiation of embryonal carcinoma cells (P19) on mitochondrial DNA content in vitro." In Vitro Cell Dev Biol **27A**(7): 557-561.

49- Vega-Naredo, I., et al. (2014). "Mitochondrial metabolism directs stemness and differentiation in P19 embryonal carcinoma stem cells." Cell Death Differ.

50- Bonnet S., Archer S. L., Allalunis-Turner J., Haromy A., Beaulieu C., Thompson R., Lee C. T., Lopaschuk G. D., Puttagunta L., Bonnet S., Harry G., Hashimoto K., Porter C. J., Andrade M. A., Thebaud B., Michelakis E. D. (2007). "A mitochondria-K+ channel axis is suppressed in cancer and its normalization promotes apoptosis and inhibits cancer growth". Cancer Cell **11**(1): 37-51.

51- Michelakis, E. D., Webster, L., Mackey, J. R. (2008). "Dichloroacetate (DCA) as a potential metabolic-targeting therapy for cancer." Br J Cancer **99**(7): 989-994.

52- Michelakis, E. D., et al. (2010). "Metabolic modulation of glioblastoma with dichloroacetate." Sci Transl Med **2**(31): 31ra34

53- Pangborn M. (1942). "Isolation and purification of a serologically active phospholipid from beef heart." J. Biol. Chem. **143**: 247–256.

54- Stoffel, W. and H. G. Schiefer (1968). "Biosynthesis and composition of phosphatides in outer and inner mitochondrial membranes." Hoppe Seylers Z Physiol Chem **349**(8): 1017-1026.

55- Haines, T. H. (2009). "A new look at Cardiolipin." Biochim Biophys Acta **1788**(10): 1997-2002.

56- Hatch, G. M. and G. McClarty (1996). "Regulation of cardiolipin biosynthesis in H9c2 cardiac myoblasts by cytidine 5'-triphosphate." J Biol Chem **271**(42): 25810-25816.

57- Schlame, M., et al. (2005). "Molecular symmetry in mitochondrial cardiolipins." Chem Phys Lipids **138**(1-2): 38-49.

58- Buckland, A. G., et al. (1998). "Cardiolipin hydrolysis by human phospholipases A2. The multiple enzymatic activities of human cytosolic phospholipase A2." Biochim Biophys Acta **1390**(1): 65-72.

59- Chicco, A. J. and G. C. Sparagna (2007). "Role of cardiolipin alterations in mitochondrial dysfunction and disease." Am J Physiol Cell Physiol **292**(1): C33-44.

60- Ruggiero, F. M. Cafagna, F. Petruzzella, V. Gadaleta, M. N. Quagliariello, E. (1992). "Lipid composition in synaptic and nonsynaptic mitochondria from rat brains and effect of aging." J Neurochem **59**(2): 487-491

61- Shidoji, Y., Hayashi, K., Komura, S., Ohishi, N., Yagi, K. (1999). "Loss of molecular interaction between cytochrome c and cardiolipin due to lipid peroxidation." Biochem Biophys Res Commun **264**(2): 343-347.

62- Sparagna G. C., Chicco A. J., Murphy R. C., Bristow M. R., Johnson C. A., Rees M. L., Srere, P. A. (1963). "Citryl-Coa. An Substrate for the Citrate-Cleavage Enzyme." Biochim Biophys Acta **73**: 523-525.

63- Han, X., Yang, J., Yang, K., Zhao, Z., Abendschein, D. R., Gross, R. W. (2007). "Alterations in myocardial cardiolipin content and composition occur at the very earliest stages of diabetes: a shotgun lipidomics study." Biochemistry **46**(21): 6417-6428.

64- Michael A. Kiebish,et al. (2008). "Cardiolipin and electron transport chain abnormalities in mouse brain tumor mitochondria: lipidomic evidence supporting the Warburg theory of cancer." J Lipid Res **49**(12): 2545–2556.

65- Barth, P. G., Scholte, H. R., Berden, J. A., Van der Klei-Van Moorsel, J. M., Luyt-Houwen, I. E., Van 't Veer-Korthof, E. T., Van der Harten, J. J., Sobotka-Plojhar, M. A. (1983). "An X-linked mitochondrial disease affecting cardiac muscle, skeletal muscle and neutrophil leucocytes." J Neurol Sci **62**(1-3): 327-355.

66- McBurney, M. W. and B. J. Rogers (1982). "Isolation of male embryonal carcinoma cells and their chromosome replication patterns." Dev Biol **89**(2): 503-508.

67- Paradies, G., et al. (2001). "Reactive oxygen species generated by the mitochondrial respiratory chain affect the complex III activity via cardiolipin peroxidation in beef-heart submitochondrial particles." Mitochondrion **1**(2): 151-159.

68- Petrosillo, G., et al. (2003). "Decreased complex III activity in mitochondria isolated from rat heart subjected to ischemia and reperfusion: role of reactive oxygen species and cardiolipin." FASEB J **17**(6): 714-716.

69- Paradies, G., et al. (2004). "Decrease in mitochondrial complex I activity in ischemic/reperfused rat heart: involvement of reactive oxygen species and cardiolipin." Circ Res **94**(1): 53-59.

70- Musatov, A. (2006). "Contribution of peroxidized cardiolipin to inactivation of bovine heart cytochrome c oxidase." Free Radic Biol Med **41**(2): 238-246.

71- Berger, A., et al. (1993). "Biochemistry of cardiolipin: sensitivity to dietary fatty acids." Adv Food Nutr Res **37**: 259-338.

72- Fry, M. and D. E. Green (1981). "Cardiolipin requirement for electron transfer in complex I and III of the mitochondrial respiratory chain." J Biol Chem **256**(4): 1874-1880.

73- Reiter, R. J., et al. (2000). "Melatonin and its relation to the immune system and inflammation." Ann N Y Acad Sci **917**: 376-386.

74- Hardeland, R., et al. (2006). "Melatonin." Int J Biochem Cell Biol **38**(3): 313-316.

75- Martin, V., et al. (2006). "Intracellular signaling pathways involved in the cell growth inhibition of glioma cells by melatonin." Cancer Res **66**(2): 1081-1088.

76- Korkmaz, A., et al. (2012). "Glucose: a vital toxin and potential utility of melatonin in protecting against the diabetic state." Mol Cell Endocrinol **349**(2): 128-137.

77- Acuna-Castroviejo, D., et al. (2007). "Melatonin role in the mitochondrial function." Front Biosci **12**: 947-963.

78- Reiter, R. J., et al. (2001). "Free radical-mediated molecular damage. Mechanisms for the protective actions of melatonin in the central nervous system." Ann N Y Acad Sci **939**: 200-215.

79- Vega-Naredo, I., et al. (2005). "Melatonin neutralizes neurotoxicity induced by quinolinic acid in brain tissue culture." J Pineal Res **39**(3): 266-275.

80- Calvo, J. R., et al. (2013). "The role of melatonin in the cells of the innate immunity: a review." J Pineal Res **55**(2): 103-120.

81- Sainz, R. M., et al. (2003). "Melatonin and cell death: differential actions on apoptosis in normal and cancer cells." Cell Mol Life Sci **60**(7): 1407-1426

82- Vega-Naredo, I., et al. (2012). "Melatonin modulates autophagy through a redox-mediated action in female Syrian hamster Harderian gland controlling cell types and gland activity." J Pineal Res **52**(1): 80-92.

83- Rodriguez, C., et al. (2013). "Mechanisms involved in the pro-apoptotic effect of melatonin in cancer cells." Int J Mol Sci **14**(4): 6597-6613.

84- Bligh, E. G. and Dyer, W. J. (1959). "A rapid method of total lipid extraction and purification." Can J Biochem Physiol **37**(8): 911-917.

85- Bartlett, G. R. (1959). "Phosphorus assay in column chromatography." J Biol Chem **234**(3): 466-468.

86- Skehan, P., et al. (1990). "New colorimetric cytotoxicity assay for anticancer-drug screening." J Natl Cancer Inst **82**(13): 1107-1112.

87- Petrosillo, G., et al. (2003). "Role of reactive oxygen species and cardiolipin in the release of cytochrome c from mitochondria." FASEB J **17**(15): 2202-2208.

88- Veenman, L., et al. (2008). "VDAC activation by the 18 kDa translocator protein (TSPO), implications for apoptosis." J Bioenerg Biomembr **40**(3): 199-205.

89- Caballero, B., et al. (2013). "Role of mitochondrial translocator protein (18 kDa) on mitochondrial- related cell death processes." Recent Pat Endocr Metab Immune Drug Discov **7**(2): 86-101.

90- Hsu, F. F., et al. (2005). "Structural characterization of cardiolipin by tandem quadrupole and multiple-stage quadrupole ion-trap mass spectrometry with electrospray ionization." J Am Soc Mass Spectrom **16**(4): 491-504.

91- Brugger, B., et al. (1997). "Quantitative analysis of biological membrane lipids at the low picomole level by nano-electrospray ionization tandem mass spectrometry." Proc Natl Acad Sci U S A **94**(6): 2339-2344.

92- Wiseman, D. A., et al. (2007). "Alterations in zinc homeostasis underlie endothelial cell death induced by oxidative stress from acute exposure to hydrogen peroxide." Am J Physiol Lung Cell Mol Physiol **292**(1): L165-177.

93- Ott, M., et al. (2002). "Cytochrome c release from mitochondria proceeds by a two-step process." Proc Natl Acad Sci U S A **99**(3): 1259-1263.

94- Petrosillo, G., et al. (2013). "Decline in cytochrome c oxidase activity in rat-brain mitochondria with aging. Role of peroxidized cardiolipin and beneficial effect of melatonin." J Bioenerg Biomembr **45**(5): 431-440.

95- Kroemer, G., et al. (2007). "Mitochondrial membrane permeabilization in cell death." Physiol Rev **87**(1): 99-163.

96- Petrosillo, G., et al. (2013). "Decline in cytochrome c oxidase activity in rat-brain mitochondria with aging. Role of peroxidized cardiolipin and beneficial effect of melatonin." J Bioenerg Biomembr **45**(5): 431-440.

97- Bejarano, I., et al. (2011). "Pro-oxidant effect of melatonin in tumour leucocytes: relation with its cytotoxic and pro-apoptotic effects." Basic Clin Pharmacol Toxicol **108**(1): 14-20.

98- Albertini, M. C., et al. (2006). "Intracellular pro-oxidant activity of melatonin deprives U937 cells of reduced glutathione without affecting glutathione peroxidase activity." Ann N Y Acad Sci **1091**: 10-16.

99- Osseni, R. A., et al. (2000). "Evidence of prooxidant and antioxidant action of melatonin on human liver cell line HepG2." Life Sci **68**(4): 387-399.

100- van den Brink-van der Laan, E., et al. (2004). "Nonbilayer lipids affect peripheral and integral membrane proteins via changes in the lateral pressure profile." Biochim Biophys Acta **1666**(1-2): 275-288.

101- Xu, F. Y., et al. (2000). "Elevation in phosphatidylethanolamine is an early but not essential event for cardiac cell differentiation." Exp Cell Res **256**(2): 358-364.

102- Chen, C. T., et al. (2008). "Coordinated changes of mitochondrial biogenesis and antioxidant enzymes during osteogenic differentiation of human mesenchymal stem cells." Stem Cells **26**(4): 960-968.

103- Tyurin, V. A., et al. (2008). "Mass-spectrometric characterization of phospholipids and their primary peroxidation products in rat cortical neurons during staurosporine-induced apoptosis." J Neurochem **107**(6): 1614-1633.

104- Jiang, J., et al. (2009). "A mitochondria-targeted triphenylphosphonium-conjugated nitroxide functions as a radioprotector/mitigator." Radiat Res **172**(6): 706-717.

105- Tyurina, Y. Y., et al. (2008). "Oxidative lipidomics of gamma-irradiation-induced intestinal injury." Free Radic Biol Med **44**(3): 299-314.

106- Bayir, H., et al. (2007). "Selective early cardiolipin peroxidation after traumatic brain injury: an oxidative lipidomics analysis." Ann Neurol **62**(2): 154-169.

107- Kagan, V. E., et al. (2005). "Cytochrome c acts as a cardiolipin oxygenase required for release of proapoptotic factors." Nat Chem Biol **1**(4): 223-232.

108- Gonzalvez, F. and E. Gottlieb (2007). "Cardiolipin: setting the beat of apoptosis." Apoptosis **12**(5): 877-885.

109- Stefanyk, L. E., et al. (2010). "Skeletal muscle type comparison of subsarcolemmal mitochondrial membrane phospholipid fatty acid composition in rat." J Membr Biol **234**(3): 207-215

110- Chen, C. T., et al. (2008). "Coordinated changes of mitochondrial biogenesis and antioxidant enzymes during osteogenic differentiation of human mesenchymal stem cells." Stem Cells **26**(4): 960-968.

111- Post, J. A., Verkleij, A. J., Langer, G. A. (1995). "Organization and function of sarcolemmal phospholipids in control and ischemic/reperfused cardiomyocytes." J Mol Cell Cardiol **27**(2): 749-760

112- Doria, M. L., et al. (2012). "Lipidomic approach to identify patterns in phospholipid profiles and define class differences in mammary epithelial and breast cancer cells." Breast Cancer Res Treat **133**(2): 635-648.

113- Bottinger, L., et al. (2012). "Phosphatidylethanolamine and cardiolipin differentially affect the stability of mitochondrial respiratory chain supercomplexes." J Mol Biol **423**(5): 677-686.

114- Pathak, S., et al. (2014). "Tafazzin protein expression is associated with tumorigenesis and radiation response in rectal cancer: a study of Swedish clinical trial on preoperative radiotherapy." PLoS One **9**(5): e98317.

115- Acehan, D., et al. (2009). "Distinct effects of tafazzin deletion in differentiated and undifferentiated mitochondria." Mitochondrion **9**(2): 86-95.

116- Petrosillo, G., et al. (2009). "Melatonin inhibits cardiolipin peroxidation in mitochondria and prevents the mitochondrial permeability transition and cytochrome c release." Free Radic Biol Med **47**(7): 969-974.

117- Garcia Fernandez, M., et al. (2002). "Early changes in intramitochondrial cardiolipin distribution during apoptosis." Cell Growth Differ **13**(9): 449-455.

118- Barbosa, I. A., et al. (2012). "Mitochondrial remodeling in cancer metabolism and survival: potential for new therapies." Biochim Biophys Acta **1826**(1): 238-254.

119- Shyh-Chang, N., et al. (2013). "Stem cell metabolism in tissue development and aging." Development **140**(12): 2535-2547.

120- Bizzarri, M., et al. (2013). "Molecular mechanisms of the pro-apoptotic actions of melatonin in cancer: a review." Expert Opin Ther Targets **17**(12): 1483-1496.

121- Cucina, A., et al. (2009). "Evidence for a biphasic apoptotic pathway induced by melatonin in MCF-7 breast cancer cells." J Pineal Res **46**(2): 172-180.

122- Joza, N., et al. (2001). "Essential role of the mitochondrial apoptosis-inducing factor in programmed cell death." Nature **410**(6828): 549-554

123- Brantley-Finley, C., et al. (2003). "The JNK, ERK and p53 pathways play distinct roles in apoptosis mediated by the antitumor agents vinblastine, doxorubicin, and etoposide." Biochem Pharmacol **66**(3): 459-469.

124- Kantrowitz, N. E. and M. R. Bristow (1984). "Cardiotoxicity of antitumor agents." Prog Cardiovasc Dis **27**(3): 195-200.

125- Hande, K. R. (1998). "Etoposide: four decades of development of a topoisomerase II inhibitor." Eur J Cancer **34**(10): 1514-1521.

PART 9

APENDIX: COPYRIGHT LICENSE AGREEMENTS

Appendix 1

NATURE PUBLISHING GROUP LICENSE TERMS AND CONDITIONS

Jul 28, 2014

This is a License Agreement between Silvia Novais ("You") and Nature Publishing Group ("Nature Publishing Group") provided by Copyright Clearance Center ("CCC"). The license consists of your order details, the terms and conditions provided by Nature Publishing Group, and the payment terms and conditions.

All payments must be made in full to CCC. For payment instructions, please see information listed at the bottom of this form.

License Number	3437631401097
License date	Jul 28, 2014
Licensed content publisher	Nature Publishing Group
Licensed content publication	Nature
Licensed content title	Stem cells, cancer, and cancer stem cells
Licensed content author	Tannishtha Reya, Sean J. Morrison, Michael F. Clarke, Irving L. Weissman
Licensed content date	Nov 1, 2001
Volume number	414
Issue number	6859
Type of Use	reuse in a dissertation / thesis
Requestor type	academic/educational
Format	print and electronic
Portion	figures/tables/illustrations
Number of figures/tables/illustrations	1
Figures	Figure 4.
Author of this NPG article	no
Your reference number	None
Title of your thesis / dissertation	The content of cardiolipin in P19 embryonic carcinoma cells
Expected completion date	Sep 2014
Estimated size (number of pages)	90
Total	0.00 EUR
Terms and Conditions	

Terms and Conditions for Permissions

Nature Publishing Group hereby grants you a non-exclusive license to reproduce this material for this purpose, and for no other use,subject to the conditions below:

1. NPG warrants that it has, to the best of its knowledge, the rights to license reuse of this material. However, you should ensure that the material you are requesting is original to Nature Publishing Group and does not carry the copyright of another entity (as credited in the published version). If the credit line on any part of the material you have requested indicates that it was reprinted or adapted by NPG with permission from another source, then you should also seek permission from that source to reuse the material.

2. Permission granted free of charge for material in print is also usually granted for any electronic version of that work, provided that the material is incidental to the work as a whole and that the electronic version is essentially equivalent to, or substitutes for, the print version.Where print permission has been granted for a fee, separate permission must be obtained for any additional, electronic re-use (unless, as in the case of a full paper, this has already been accounted for during your initial request in the calculation of a print run).NB: In all cases, web-based use of full-text articles must be authorized separately through the 'Use on a Web Site' option when requesting permission.

3. Permission granted for a first edition does not apply to second and subsequent editions and for editions in other languages (except for signatories to the STM Permissions Guidelines, or where the first edition permission was granted for free).

4. Nature Publishing Group's permission must be acknowledged next to the figure, table or abstract in print. In electronic form, this acknowledgement must be visible at the same time as the figure/table/abstract, and must be hyperlinked to the journal's homepage.

5. The credit line should read:
Reprinted by permission from Macmillan Publishers Ltd: [JOURNAL NAME] (reference citation), copyright (year of publication)
For AOP papers, the credit line should read:
Reprinted by permission from Macmillan Publishers Ltd: [JOURNAL NAME], advance online publication, day month year (doi: 10.1038/sj.[JOURNAL ACRONYM].XXXXX)

   Note: For republication from the *British Journal of Cancer*, the following credit lines apply.
Reprinted by permission from Macmillan Publishers Ltd on behalf of Cancer Research UK: [JOURNAL NAME] (reference citation), copyright (year of publication)For AOP papers, the credit line should read:
Reprinted by permission from Macmillan Publishers Ltd on behalf of Cancer Research UK: [JOURNAL NAME], advance online publication, day month year (doi: 10.1038/sj.[JOURNAL ACRONYM].XXXXX)

6. Adaptations of single figures do not require NPG approval. However, the adaptation should be credited as follows:

   Adapted by permission from Macmillan Publishers Ltd: [JOURNAL NAME] (reference citation), copyright (year of publication)

   Note: For adaptation from the *British Journal of Cancer*, the following credit line applies.
Adapted by permission from Macmillan Publishers Ltd on behalf of Cancer Research UK: [JOURNAL NAME] (reference citation), copyright (year of publication)

7. Translations of 401 words up to a whole article require NPG approval. Please visit http://www.macmillanmedicalcommunications.com for more information.Translations of up to a 400 words do not require NPG approval. The translation should be credited as follows:

   Translated by permission from Macmillan Publishers Ltd: [JOURNAL NAME] (reference citation), copyright (year of publication).

   Note: For translation from the *British Journal of Cancer*, the following credit line applies.
Translated by permission from Macmillan Publishers Ltd on behalf of Cancer Research UK: [JOURNAL NAME] (reference citation), copyright (year of publication)

We are certain that all parties will benefit from this agreement and wish you the best in the use of this material. Thank you.

Special Terms:

v1.1

You will be invoiced within 48 hours of this transaction date. You may pay your invoice by credit card upon receipt of the invoice for this transaction. Please follow instructions provided at that time.
To pay for this transaction now; please remit a copy of this document along with your payment. Payment should be in the form of a check or money order referencing your account number and this invoice number RLNK501362927.
Make payments to "COPYRIGHT CLEARANCE CENTER" and send to:

Copyright Clearance Center
Dept 001
P.O. Box 843006
Boston, MA 02284-3006
Please disregard electronic and mailed copies if you remit payment in advance.
Questions? customercare@copyright.com or +1-855-239-3415 (toll free in the US) or +1-978-646-2777.

Gratis licenses (referencing $0 in the Total field) are free. Please retain this printable license for your reference. No payment is required.

Appendix 2

NATURE PUBLISHING GROUP LICENSE TERMS AND CONDITIONS

Jul 22, 2014

This is a License Agreement between Silvia Novais ("You") and Nature Publishing Group ("Nature Publishing Group") provided by Copyright Clearance Center ("CCC"). The license consists of your order details, the terms and conditions provided by Nature Publishing Group, and the payment terms and conditions.

All payments must be made in full to CCC. For payment instructions, please see information listed at the bottom of this form.

License Number	3434110412462
License date	Jul 22, 2014
Licensed content publisher	Nature Publishing Group
Licensed content publication	Cell Death and Differentiation
Licensed content title	Mitochondrial metabolism directs stemness and differentiation in P19 embryonal carcinoma stem cells
Licensed content author	I Vega-Naredo, R Loureiro, K A Mesquita, I A Barbosa, L C Tavares, A F Branco, J R Erickson, J Holy, E L Perkins, R A Carvalho, P J Oliveira
Licensed content date	May 16, 2014
Volume number	0
Issue number	0
Type of Use	reuse in a dissertation / thesis
Requestor type	academic/educational
Format	print and electronic
Portion	figures/tables/illustrations
Number of figures/tables/illustrations	4
High-res required	no
Figures	Supplementary figure s1 Figure 3 Figure 6 Figure 7
Author of this NPG article	no
Your reference number	None
Title of your thesis / dissertation	The content of cardiolipin in P19 embryonic carcinoma cells
Expected completion date	Sep 2014
Estimated size (number of pages)	90
Total	0.00 EUR
Terms and Conditions	

Terms and Conditions for Permissions

Nature Publishing Group hereby grants you a non-exclusive license to reproduce this material for this purpose, and for no other use,subject to the conditions below:

1. NPG warrants that it has, to the best of its knowledge, the rights to license reuse of this material. However, you should ensure that the material you are requesting is original to Nature Publishing Group and does not carry the copyright of another entity (as credited in the published version). If the credit line on any part of the material you have requested indicates that it was reprinted or adapted by NPG with permission from another source, then you should also seek permission from that source to reuse the material.

2. Permission granted free of charge for material in print is also usually granted for any electronic version of that work, provided that the material is incidental to the work as a whole and that the electronic version is essentially equivalent to, or substitutes for, the print version.Where print permission has been granted for a fee, separate permission must be obtained for any additional, electronic re-use (unless, as in the case of a full paper, this has already been accounted for during your initial request in the calculation of a print run).NB: In all cases, web-based use of full-text articles must be authorized separately through the 'Use on a Web Site' option when requesting permission.

3. Permission granted for a first edition does not apply to second and subsequent editions and for editions in other languages (except for signatories to the STM Permissions Guidelines, or where the first edition permission was granted for free).

4. Nature Publishing Group's permission must be acknowledged next to the figure, table or abstract in print. In electronic form, this acknowledgement must be visible at the same time as the figure/table/abstract, and must be hyperlinked to the journal's homepage.

5. The credit line should read:
   Reprinted by permission from Macmillan Publishers Ltd: [JOURNAL NAME] (reference citation), copyright (year of publication)
   For AOP papers, the credit line should read:
   Reprinted by permission from Macmillan Publishers Ltd: [JOURNAL NAME], advance online publication, day month year (doi: 10.1038/sj.[JOURNAL ACRONYM].XXXXX)

   Note: For republication from the *British Journal of Cancer*, the following credit lines apply.
   Reprinted by permission from Macmillan Publishers Ltd on behalf of Cancer Research UK: [JOURNAL NAME] (reference citation), copyright (year of publication)For AOP papers, the credit line should read:
   Reprinted by permission from Macmillan Publishers Ltd on behalf of Cancer Research UK: [JOURNAL NAME], advance online publication, day month year (doi: 10.1038/sj.[JOURNAL ACRONYM].XXXXX)

6. Adaptations of single figures do not require NPG approval. However, the adaptation should be credited as follows:

   Adapted by permission from Macmillan Publishers Ltd: [JOURNAL NAME] (reference citation), copyright (year of publication)

   Note: For adaptation from the *British Journal of Cancer*, the following credit line applies.
   Adapted by permission from Macmillan Publishers Ltd on behalf of Cancer Research UK: [JOURNAL NAME] (reference citation), copyright (year of publication)

7. Translations of 401 words up to a whole article require NPG approval. Please visit http://www.macmillanmedicalcommunications.com for more information.Translations of up to a 400 words do not require NPG approval. The translation should be credited as follows:

   Translated by permission from Macmillan Publishers Ltd: [JOURNAL NAME] (reference citation), copyright (year of publication).

   Note: For translation from the *British Journal of Cancer*, the following credit line applies.
   Translated by permission from Macmillan Publishers Ltd on behalf of Cancer Research UK: [JOURNAL NAME] (reference citation), copyright (year of publication)

We are certain that all parties will benefit from this agreement and wish you the best in the use of this material. Thank you.

Special Terms:

v1.1

If you would like to pay for this license now, please remit this license along with your payment made payable to "COPYRIGHT CLEARANCE CENTER" otherwise you will be invoiced within 48 hours of the license date. Payment should be in the form of a check or money order referencing your account number and this invoice number 501357784. Once you receive your invoice for this order, you may pay your invoice by credit card. Please follow instructions provided at that time.

Make Payment To:
Copyright Clearance Center
Dept 001
P.O. Box 843006
Boston, MA 02284-3006

For suggestions or comments regarding this order, contact RightsLink Customer Support: customercare@copyright.com or +1-877-622-5543 (toll free in the US) or +1-978-646-2777.

Gratis licenses (referencing $0 in the Total field) are free. Please retain this printable license for your reference. No payment is required.

Appendix 3

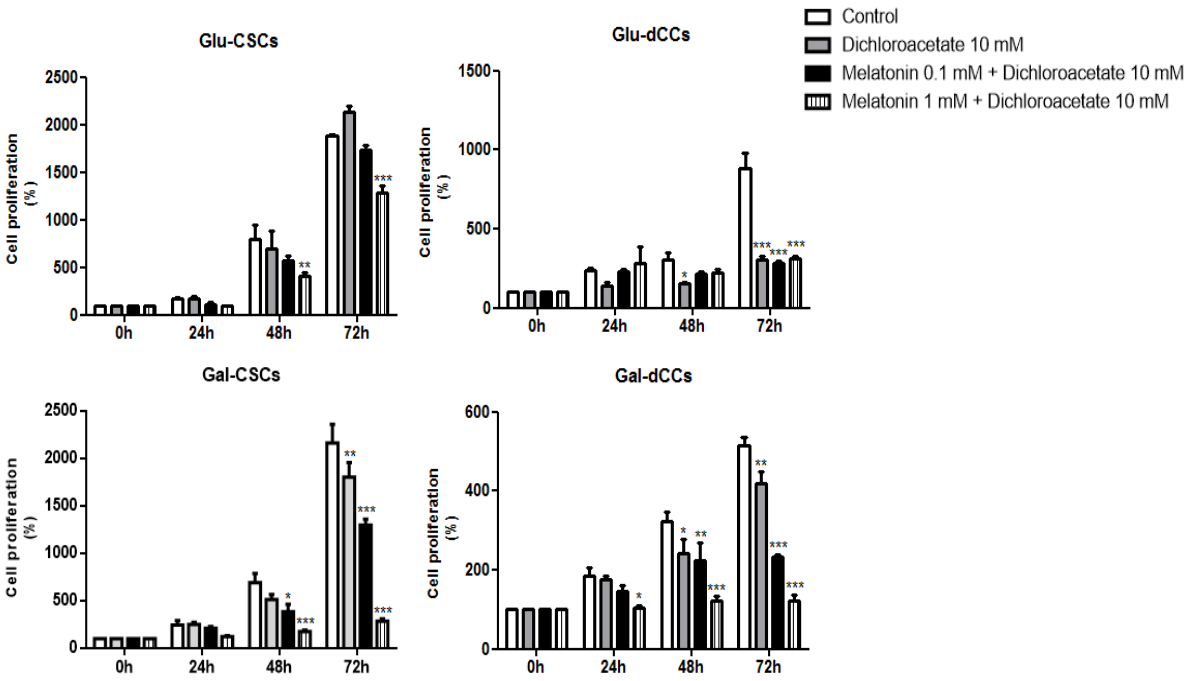

Effect of the combined treatment with melatonin and dichloroacetate (DCA) on cell viability of P19 embryonal carcinoma stem (CSCs) and differentiated (dCCs) cells, grown in glucose (Glu) and galatose (Gal) media. The sulforhodamine B (SRB) assay shows a cytotoxic effect in Glu-CSCs after 72 hours of the combined treatment with 1mM melatonin and 10 mM dichloroacetate. Data represent the average percentage of SRB absorbance with respective time 0 ± SEM from at least four independent experiments. Data are optical density (O.D.) expressed as percentage of control ± SEM from three separate immunoblots. * $p<0.05$; ** $p<0.01$; *** $p<0.001$ vs.control.